AD-A041 665 CATHOLIC UNIV OF AMERICA WASHINGTON D C VITREOUS STA--ETC F/G 11/8
DYNAMICAL SHEAR AND STRUCTURAL VISCOELASTICITY IN ELASTOHYDRODY--ETC(U)
JUL 77 C J MONTROSE, C T MOYNIHAN, H SASABE N00014-75-C-8056

UNCLASSIFIED NL

| OF |
AD
A041665

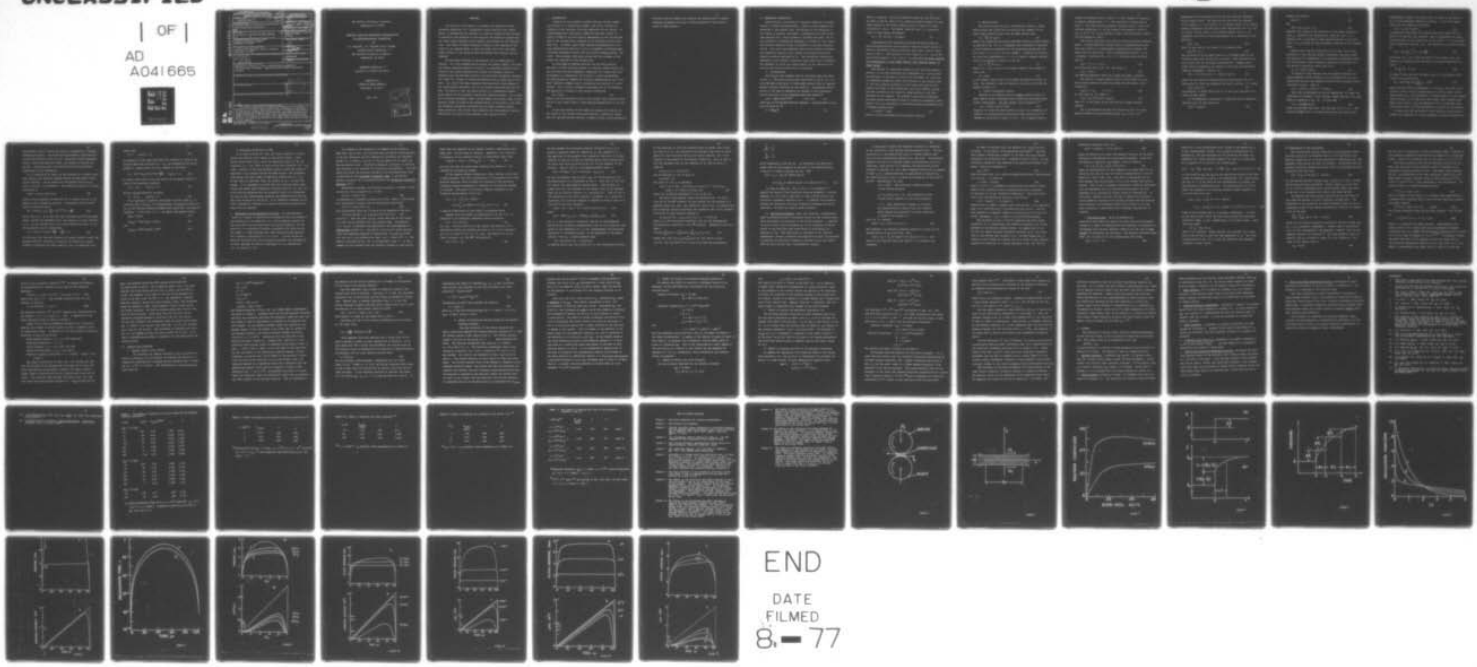

END

DATE
FILMED
8-77

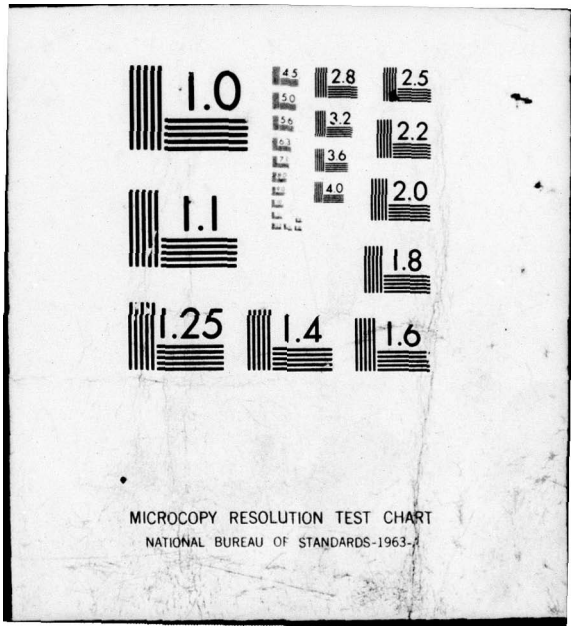
1.0
1.1
1.25
1.4
1.6
1.8
2.0
2.2
2.5
2.8
3.2
3.6
4.0
4.5
5.0
5.6
MICROCOPY RESOLUTION TEST CHART
NATIONAL BUREAU OF STANDARDS-1963-A

Unclassified

SECURITY CLASSIFICATION OF THIS PAGE (When Data Entered)

REPORT DOCUMENTATION PAGE

READ INSTRUCTIONS BEFORE COMPLETING FORM

1. REPORT NUMBER: Technical Report #6

2. GOVT ACCESSION NO.

3. RECIPIENT'S CATALOG NUMBER

4. TITLE (and Subtitle): "Dynamical Shear and Structural Viscoelasticity in Elastohydrodynamic Lubrication",

5. TYPE OF REPORT & PERIOD COVERED: Technical Report, Rept. no. 6, 2/76-6/77

6. PERFORMING ORG. REPORT NUMBER: Feb 76 - June 77

7. AUTHOR(s): C.J. Montrose, C.T. Moynihan and H. Sasabe

8. CONTRACT OR GRANT NUMBER(s): N00014-75-C-8056, NR 22-007

9. PERFORMING ORGANIZATION NAME AND ADDRESS: Catholic University of America, Washington, DC 20064

10. PROGRAM ELEMENT, PROJECT, TASK AREA & WORK UNIT NUMBERS

11. CONTROLLING OFFICE NAME AND ADDRESS: Vitreous State Laboratory, Catholic University, Washington, DC 20064

12. REPORT DATE: July 1977

13. NUMBER OF PAGES: 60

14. MONITORING AGENCY NAME & ADDRESS (if different from Controlling Office): 61 p.

15. SECURITY CLASS. (of this report): Unclassified

15a. DECLASSIFICATION/DOWNGRADING SCHEDULE

16. DISTRIBUTION STATEMENT (of this Report)

Reproduction in whole or in part is permitted for any purpose of the United States Government. Approved for public release, distribution unlimited.

17. DISTRIBUTION STATEMENT (of the abstract entered in Block 20, if different from Report)

18. SUPPLEMENTARY NOTES

19. KEY WORDS (Continue on reverse side if necessary and identify by block number)

20. ABSTRACT (Continue on reverse side if necessary and identify by block number)

The thrust of this paper is to address the question of what dynamical properties of a viscoelastic liquid lubricant are instrumental in determining the traction in a heavily loaded rolling contact. In examining this question we first explore the dynamical changes that the large normal stresses in the contact zone produce in the lubricant film.* The effect of these structural changes on the response of the liquid to the imposed shear is then evaluated; from this, the shear stress profile in the contact--which determines the traction --can be computed.

DD FORM 1 JAN 73 1473 EDITION OF 1 NOV 65 IS OBSOLETE

Unclassified

SECURITY CLASSIFICATION OF THIS PAGE (When Data Entered)

* are affected

The Catholic University of America

Washington, DC 20064

DYNAMICAL SHEAR AND STRUCTURAL VISCOELASTICITY IN ELASTOHYDRODYNAMIC LUBRICATION

by

C.J. Montrose, C.T. Moynihan and H. Sasabe

Vitreous State Laboratory

The Catholic University of America

Washington, DC 20064

TECHNICAL REPORT NO. 6

Contract No. N00014-75-C-8056

submitted to

OFFICE OF NAVAL RESEARCH

Arlington, Va 22217

July, 1977

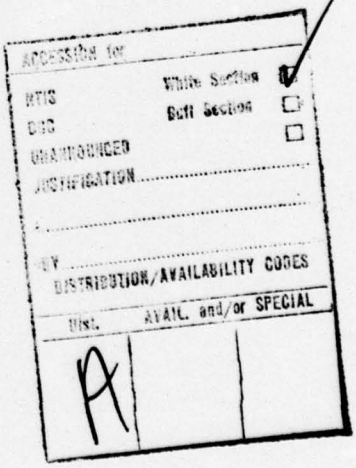

ABSTRACT

The thrust of this paper is to address the question of what dynamical properties of a viscoelastic liquid lubricant are instrumental in determining the traction in a heavily loaded rolling contact. In examining this question we first explore the dynamical changes that the large normal stresses in the contact zone produce in the lubricant film. The effect of these structural changes on the response of the liquid to the imposed shear is then evaluated; from this, the shear stress profile in the contact--which determines the traction--can be computed.

The principal features of the behavior can be summarized as follows. As a fluid element moves through the contact region, the large and rapidly changing pressure to which it is subjected produces alterations of the liquid structure that reduce the molecular mobility. Depending upon the detailed nature of the structural relaxation dynamics, this leads to a glassy or solid-like behavior over at least part of the zone. As a result the shear response characteristics (which depend on the instantaneous structure) vary as the element moves through the contact. The effect is that the stress profile is intermediate between those typical of low viscosity liquids and amorphous solids. For a given set of external variables (load, rolling speed) the initial slope of the traction curves is found to be governed mainly by the forms of the shear and structural relaxation functions and the shear rigidity modulus. Other properties such as the inlet viscosity and the pressure-viscosity coefficient are found to play somewhat less important roles.

I. INTRODUCTION

Traction is the transfer of power from one rolling element (the driver) to a second such element (the slave) through the shearing of the lubricant film that separates the two pieces. In elastohydrodynamic lubrication (EHDL) the lubricant contact is heavily loaded so that the elastic deformation of the rolling members is not insignificant compared to the thickness of the lubricant film. In recent years, EHDL theory has progressed to a rather sophisticated stage but as yet is incapable of yielding quantitatively meaningful results for the traction between driver and slave. The principal difficulty arises when one attempts to describe the lubricant in the contact zone.

In this paper we address directly the two-fold question: How does a liquid lubricant behave in a heavily loaded rolling contact and what are the fundamental properties of a liquid that are instrumental in determining the traction in such circumstances. For definiteness we examine the situation exemplified by the "twin-disk" apparatus commonly used in measuring the traction in a line contact. Fig. 1 gives a schematic representation of the geometry. The quantity of interest is the traction coefficient

$$C_T = F_t/F_n \qquad (1)$$

where F_t is the tangential force in the contact (the tractive force) and F_n is the normal force or load exerted perpendicular to the contact.

In the next section of this paper we analyze the behavior of the liquid in the contact zone and establish a theoretical framework for calculating the traction in terms of basic liquid properties.

Following this we compute the traction for several sets of typical lubricant parameters and give a brief discussion of the significance of these results.

II THEORETICAL FORMULATION

Qualitatively, the picture of lubricant behavior in an EHDL contact is rather straightforward. Under the high pressures experienced in the contact zone, the mobility of the molecules in the liquid is severely restricted. Consequently for much of the time required for a fluid element to traverse this zone, the liquid structure is dynamically arrested or "frozen in; as a result the lubricant exhibits glassy or amorphous solid-like characteristics. This solid pad separating the rolling elements transmits the tangential traction force through the essentially elastic shearing stresses developed in it. The theoretical formulation developed in this section translates these ideas into a mathematical framework by which the stress profile in the lubricant film and thus the tractive force can be calculated.

1. Preliminaries

The contact zone geometry and the coordinate axes are shown in Fig. 2. The disks rolling with velocities U_1 and U_2 ($U_1 > U_2$) have deformed elastically to form an EHDL contact zone of (approximately) constant thickness 2h and width 2b. The pressure distribution in the zone is assumed to be uniform in the y-direction and to vary with x as an elliptical Hertzian profile[1]

$$p(x) = P_{HZ}[1-(x/b)^2]^{1/2} \qquad (|x| \leq b), \qquad (2)$$

where P_{HZ} is the maximum Hertzian pressure. The half-width of the zone is given by [2]

$$b = 4RP_{HZ}/E, \qquad (3)$$

where $R = R_1R_2/(R_1 + R_2)$ is an effective radius for the disk pair of radii R_1 and R_2. Here E is an effective elastic modulus for the disks related to the Young's modulus E_0 by $E = E_0/(1-\nu^2)$ where ν is Poisson's ratio. The normal force per unit (z - direction) length is thus easily calculated:

$$f_n = \int_{-b}^{b} dx\, p(x) = \pi b\, P_{HZ}/2. \qquad (4)$$

Understanding and calculating traction basically means explaining quantitatively the so-called "traction curves"--plots of traction coefficient versus slide-roll ratio $\Delta U/U$-- such as those shown in Fig. 3. The sliding (or slip) speed $\Delta U = U_1 - U_2$ and the mean rolling speed $U = (U_1 + U_2)/2$. In this paper we shall restrict our consideration to the linear portion (the low-slip region) of these curves.

The analysis is simplified further by the following approximations: (1) All the quantities are independent of z, the co-ordinate parallel to the axes of rotation of the disks; (2) there are no temperature gradients within the lubricant in the contact zone; (3) the only velocity gradients in the liquid that must be considered are those in the y-direction; and (4) all effects arising from the curvature of the disks or irregularities in the film thickness can be ignored. The problem is thus one of computing the shear stress distribution within a liquid of rectangular cross-section (2b x 2h) subjected to a Hertzian pressure distribution and a constant shearing rate

$$\dot{\varepsilon} = \partial u/\partial y = U/2h, \qquad (5)$$

where u is the x-component of the particle velocity.

2. Tractive Force

The tractive force per unit (z-direction) length f_t transferred across the liquid film is given by the integral of the shear stress profile $\sigma_{yx}(x)$ over the EHDL contact zone:

$$f_t = \int_{-b}^{+b} dx\ \sigma_{yx}(x). \tag{6}$$

Rather than examining the entire lubricant film at a fixed instant, as implied by Eq. (6), it is somewhat more convenient to consider a fluid element of dimensions dx ×2h travelling through the contact (from x = -b to x = +b) at a speed U. Formally this amounts to using the transformation x → -b + Ut (where x locates the position of the element at time t) in Eq. (6):

$$f_t = U \int_0^{t_0} dt\ \sigma(t), \tag{7}$$

where $\sigma(t) = \sigma_{yx}(-b + Ut)$ is the shear stress on the element at time t and

$$t_0 = 2b/U \tag{8}$$

is the transit time of the fluid element through the contact region. The problem is thus to construct the form of the time dependent stress $\sigma(t)$.

3. Linear Viscoelastic Theory

Because we are dealing only with <u>small</u> shearing rates, we shall employ linear viscoelasticity to describe the shear stress-strain relationship. The most general form allowable is[3]

$$\sigma(t) = \int_0^t dt'\ \Phi_s(t-t')\dot{\varepsilon}(t'). \tag{9}$$

Equation (9) gives the shear stress at time t as a summation (or integral) of contributions arising from shear strains $\dot{\varepsilon}(t')dt'$ imposed on the fluid at times $0 \leq t' \leq t$ (it is assumed that no

strains are present prior to time $t' = 0$ and, because of causality no strains imposed after $t' = t$ can contribute to the stress at time t). The shear stress relaxation function $\Phi_s(t-t')$ gives the relative weightings at t of the various contributions; that is, $\Phi_s(t-t')\dot{\varepsilon}(t')\,dt'$ is the stress at time t resulting from a strain $\dot{\varepsilon}(t')dt'$ imposed at time t'.

This can be clarified a bit more by examining several familiar cases. A simple Newtonian viscous fluid is characterized by the fact that there is an instantaneous proportionality between the stress and the shear rate. This is expressed by writing Φ_s as a constant η multiplied by $\delta(t - t')$, the Dirac delta-function; that is

$$\Phi_s(t - t') = \eta\,\delta(t-t'). \tag{10}$$

If we use this form in Eq. (9), the result is

$$\sigma(t) = \eta\dot{\varepsilon}(t), \tag{11}$$

the familiar Newtonian form with η being the shear viscosity.

The case of a linear elastic solid in which there is a constant proportionality between the stress and the strain is described by

$$\Phi_s(t-t') = G_\infty \qquad (t \geqslant t'). \tag{12}$$

In this case Eq. (9) leads to

$$\sigma(t) = G_\infty \int_0^t dt'\,\dot{\varepsilon}(t') = G_\infty\varepsilon(t). \tag{13}$$

Here $\varepsilon(t)$ is the shear strain and thus G_∞ is shear rigidity modulus.

For a viscoelastic material the form of $\Phi_s(t-t')$ is intermediate between the instantaneous decay ($\Phi_s = 0$ for $t > t'$)

appropriate for the Newtonian fluid and the constancy exhibited for an elastic solid. The form must be such that the response of the system, i.e., the stress, to an applied strain is (a) purely elastic immediately following the strain application ($t-t' \to 0$), and (b) purely viscous after a long time has passed ($t-t' \to \infty$). To accomodate the first of these requirements is is sufficient to demand that

$$\Phi_s(0) = G_\infty, \tag{14}$$

while to take care of the second, it is necessary that

$$\Phi_s(t-t' \to \infty) \to 0. \tag{15}$$

The vanishing of Φ_s at large values of its argument must be sufficiently rapid that $\int_0^t dt' \Phi_s(t')$ is finite. That this must be so can be seen from the following considerations. Suppose that a shear rate $\dot{\varepsilon}$ is imposed on the system at time zero and maintained constant thereafter. From Eq. (9)

$$\sigma(t) = \dot{\varepsilon} \int_0^t dt' \Phi_s(t-t') = \dot{\varepsilon} \int_0^t dt'' \Phi_s(t''), \tag{16}$$

where the last equality follows from the substitution $t'' = t-t'$. Taking the $t \to \infty$ limit and comparing the result with Eq. (11) yields

$$\int_0^\infty dt \Phi_s(t) = \eta; \tag{17}$$

the integral is indeed finite and is in fact just the shear viscosity of the liquid.

It is convenient to construct a normalized stress relaxation function $\phi_s(t)$ by the definition

$$\Phi_s(t) \equiv G_\infty \phi_s(t). \tag{18}$$

clearly this implies

$$\phi_s(o) = 1 \tag{19}$$

and

$$\int_0^\infty dt\ \phi_s(t) = \eta/G_\infty \equiv \tau_s \tag{20}$$

Equation (20) serves as the definition of the shear relaxation time τ_s. Recalling the normalization condition (19), it is apparent that τ_s provides a rough characterization of the time scale for ϕ_s to decay by some significant fraction of its original value.

Observe also that the definition of τ_s in Eq. (20) is the equivalent of the familiar Maxwell relaxation time even though the definition is independent of any specific viscoelastic model. The usual Maxwell single relaxation equations are obtained for the specific exponential decay form of ϕ_s:

$$\phi_s\ (t) = \exp\ (-tG_\infty/\eta). \tag{21}$$

In passing we also observe that the commonly employed frequency dependent shear viscosity $\eta(\omega)$ and modulus $G(\omega)$ are obtained from the real and imaginary parts of the one-sided Fourier transform of $\phi_s(t)$. That is,

$$\eta(\omega) - iG(\omega)/\omega = \int_o^\infty dt\ e^{-i\omega t}\ \phi_s(t). \tag{22}$$

With this as background we can now examine Eq. (9) under the conditions of interest in this problem, namely when $\dot{\epsilon}(t)$ is a constant as indicated in Eq. (5). In this case

$$\sigma(t) = \dot{\epsilon} G_\infty \int_o^t dt" \phi_s(t") \tag{23}$$

where we have made use of Eq. (18) and have let $t" = t-t'$. The quantity $G_\infty \int_o^t dt" \phi_s(t")$ is clearly seen to be the ratio of the

instantaneous stress to the shear rate; as such, we can think of it as a time dependent effective viscosity. It is to be emphasized that this effective viscosity,

$$\mu(t) \equiv G_\infty \int_o^t dt" \Phi_s(t"), \tag{24}$$

is meaningful only under the constant shear rate conditions for which it is defined, and, moreover, that it approaches the actual "true"viscosity of the liquid only in the limit $t \to \infty$ as is evident from a comparison with Eq. (17). The formula for f_t can be written as

$$f_t = (Ut_o)\left[\frac{1}{t_o}\int_o^{t_o} dt\ \mu(t)\right]\left(\frac{\Delta U}{2h}\right). \tag{25}$$

The factor $Ut_o = 2b$ is just the width of the contact zone; the quantity in brackets can be defined as an average effective viscosity

$$\bar{\mu} \equiv \frac{1}{t_o}\int_o^{t_o} dt\ \mu(t). \tag{26}$$

In terms of this and with the help of Eq.(4), the traction coefficient can be written as

$$C_T = (2b/\pi h P_{HZ})\left[G_\infty\left(\frac{\bar{\mu}}{\frac{1}{2}G_\infty t_o}\right)\right] \quad (\Delta U/U). \tag{27}$$

Apart from the external parameters b, h and P_{HZ}, the slope of the traction curves (Fig.3)is proportional to (but not equal to)the shear modulus G_∞. The coefficient of proportionality is the dynamic factor $\bar{\mu}/\frac{1}{2}G_\infty t_o$; as we shall see, this factor never exceeds unity. Notice that since $b \propto P_{HZ}$ the dependence of C_T on Hertzian pressure arises solely from the dependence of G_∞ and $\bar{\mu}$ on the pressure.

At this point the calculation of the tractive force would be essentially completed if it were possible to ignore the effects of

the pressure pulse to which the liquid is subjected as it passes through the contact. One would use the (presumably known) value of G_∞ and the functional form of $\phi_s(t)$, determined either experimentally or from some molecular model, and compute the stress via Eq.(23). This being done, the tractive force and the traction coefficient follow immediately.

It is instructive to carry out this program for a simple situation ignoring the pressure induced effects as some useful limits can be obtained. Let us assume that the Maxwell form of $\phi_s(t)$ given in Eq.(21) is appropriate. The effective viscosity is easily calculated as

$$\mu_M(t) = G_\infty \tau_s [1-\exp(-t/\tau_s)] \tag{28}$$

where we have appended the subscript "M" to denote the use of the Maxwell stress relaxation function. Multiplying this by $\dot{\varepsilon} = U/2h$ gives the tractive force:

$$f_t = (Ut_o)\{G_\infty \tau_s [1- \frac{\tau_s}{t_o} (1-e^{-t_o/\tau_s})]\} (\frac{\Delta U}{2h}). \tag{29}$$

Notice that $Ut_o = 2b$ so that the only variation with rolling speed enters through the dependence of $\bar{\mu}$, the quantity in curly brackets, on t_o. At low viscosities or low rolling speeds such that $\tau_s << t_o$, the exponential can be ignored and

$$f_t \simeq (2b)[\eta(1-\tau_s/t_o)] (\frac{\Delta U}{2h}). \quad (\frac{t_o}{\tau_s} >> 1) \tag{30}$$

In this limit the lubricant behaves as a simple viscous liquid. The average effective viscosity is given by the quantity in square brackets; neglecting the small quantity τ_s/t_o in comparison with

unity gives

$$\bar{\mu} \simeq \eta \qquad (t_o/\tau_s >> 1) \tag{31}$$

as expected. On the other hand when the viscosity is large or the rolling speed high such that $\tau_s >> t_o$, the exponential can be expanded in a power series in t_o/τ_s leading to the result

$$f_t \simeq (2b)[\tfrac{1}{2} G_\infty t_o(1-t_o/3\tau_s)](\frac{\Delta U}{2h}). \qquad (t_o/\tau_s << 1) \tag{32}$$

To lowest order this is just the result for an elastic solid; in terms of the effective viscosity

$$\mu(t) \simeq G_\infty t, \qquad (t_o/\tau_s << 1) \tag{33}$$

and the average effective viscosity

$$\bar{\mu} \simeq \tfrac{1}{2} G\, t_o. \qquad (t_o/\tau_s << 1) \tag{34}$$

It is important to observe from Eq.(29) that for fixed t_o, f_t (and thus also $\bar{\mu}$ and C_T) is a monotonically increasing function of τ_s; as the lubricant behavior becomes more solid-like, the traction increases. In the limit $\tau_s \to \infty$, we obtain the maximum values:

$$\bar{\mu}_{max} = \tfrac{1}{2} G_\infty t_o; \tag{35}$$

$$f_{t,max} = (2b)[\tfrac{1}{2} G_\infty t_o](\Delta U/2h); \tag{36}$$

and

$$C_{T,max} = (2b/\pi h\, P_{HZ}) G_\infty\, (\Delta U/U). \tag{37}$$

4. Structural Relaxation in EHDL

It is clear from Eq. (27) that the crucial quantity in determining the traction curve slopes is the factor $\bar{\mu}/\frac{1}{2}G_\infty t_o$. This factor varies from $2\tau_s/t_o$, which is essentially zero, in the low viscosity ($\tau_s << t_o$) limit to unity in the high viscosity ($\tau_s >> t_o$) limit. Because of the large pressure pulse to which the liquid is subjected in its passage through the EHDL contact, the relaxation time varies over many orders of magnitude ranging from $\tau_s << t_o$ at the inlet to (and exit from) the contact to $\tau_s >> t_o$ near the center. It is necessary to account for this variation when calculating the stress and/or effective viscosity from Eq. (23) and (24). To do this we recognize that the relaxation time τ_s is determined not only by the instantaneous pressure and temperature but also by the local structure of the fluid. It is therefore necessary to devise a theoretical fomulation in terms of which the structural dynamics can be computed.

A. Description of the Dynamical Structure. The thermodynamic state of a system in equilibrium is determined when the pressure P and temperature T are specified (in a multi-component system one must also give the concentrations of the various species). We suppose that it is possible to define a parameter--for which we use the symbol ξ --that describes the local structure of the material. For a system in equilibrium $\xi = \bar{\xi} = \Xi(P,T)$. In what follows we shall be concerned only with isothermal processes and consequently we shall suppress the explicit dependence of ξ on temperature; e.g., we write $\bar{\xi} = \Xi(P)$.

If a change in the pressure ΔP is imposed on the system at some time, say at $t=t_1$, the structure does not adjust instantaneously to the new conditions and thus immediately following the impressed change $\xi(t) \neq \Xi(P+\Delta P)$; only as $t \to \infty$ can we expect $\xi(t)$ to reach its new equilibrium value. Practically speaking, of course, an infinite time interval is not required for structural equilibration. The time scale over which the structure relaxes to its new equilibrium value is described by the structural relaxation time, τ, and the dynamical evolution of ξ is characterized by the structural relaxation function $\phi(t/\tau)$.

Specifically consider the following situation. A system in equilibrium for $t<t_1$ at pressure P_o, so that

$$\xi(t<t_1) = \Xi(P_o) \equiv \xi_o, \tag{38}$$

is subjected to a pressure increase ΔP at $t=t_1$. When $t \to \infty$ the system will equilibrate at $P_o+\Delta P$, the new equilibrium value being

$$\xi(t \to \infty) = \Xi(P_o + \Delta P) \equiv \xi_\infty . \tag{39}$$

The instantaneous value of ξ is given by an equation of the form

$$\xi(t)=\xi_o+\gamma(\xi_\infty-\xi_o) + (1-\gamma)(\xi_\infty-\xi_o)\{1-\phi[(t-t_1)/\tau]\}, \tag{40}$$

with $0 \leq \gamma \leq 1$. Here the term $\gamma(\xi_\infty-\xi_o)$ gives that part of the change in ξ that occurs promptly with the pressure step. The quantity $(1-\gamma)(\xi_\infty-\xi_o)$ is therefore the magnitude of the time-dependent or relaxational change in ξ. The factor $1-\phi[(t-t_1)/\tau]$ gives the specific time dependent approach to equilibrium. As with ϕ_s [cf. Eqs. (15) and (19)], ϕ is normalized so that $\phi(0) = 1$ and $\phi(\infty) = 0$. The behavior described by Eq. (40) is illustrated in Fig. 4. In this example we have presumed that the pressure increase is sufficiently

small that the response can be treated linearly; specifically this means that τ can be taken as constant. Regarding τ as a function of pressure, we are assuming that ΔP is sufficiently small that

$$\tau(P_o+\Delta P) = \tau(P_o) + (\partial\tau/\partial P)_{P_o}\Delta P + \ldots \simeq \tau(P_o), \qquad (41)$$

and thus one need not worry about computing the change in τ occasioned by the pressure change.

If the imposed pressure changes are large, such as is the case in EHDL contacts, then this linearization is not possible and a more detailed analysis, which includes the changing of the structural relaxation dynamics themselves in response to the pressure changes, is required. The result of this more complete treatment is the following generalization of Eq.(40):

$$\xi(t) = \xi_o + \gamma\int_{t_1}^{t} dt' \,(d\bar{\xi}/dt') + (1-\gamma)\int_{t_1}^{t} dt'(d\bar{\xi}/dt')\{1-\phi[\int_{t_1}^{t} dt''/\tau(t'')]\}. \qquad (42)$$

A heuristic derivation of this result is presented below.

Suppose that the system (in equilibrium at P_o for $t<t_1$) is subjected to an externally impressed pressure variation

$$P(t) = P_o + p(t-t_1) \qquad (43)$$

for $t\geq t_1$. For any time $t>t_1$ we may analyze the behavior in an approximate fashion by dividing the time t_1 to t into N intervals by a set of "cuts" at t_2, $t_3 \ldots t_k \ldots t_N$. The duration of any of these intervals, e.g. the $k^{\underline{th}}$, is denoted by

$$\Delta t_k = t_{k+1} - t_k. \qquad (44)$$

We also replace the continuous pressure variation $p(t-t_1)$ by a series of pressure steps ΔP_1 imposed at t_1, ΔP_2 imposed at t_2... The amplitude of the pressure step imposed at the start of a given interval is such as to make the pressure during that interval have the value that would be given by Eq.(43) for the midpoint of the interval. Thus at time t_k, the imposed pressure step is

$$\Delta P_k = p[\tfrac{1}{2}(t_{k+1} + t_k) - t_1] - p[\tfrac{1}{2}(t_k + t_{k-1}) - t_1] \qquad (45)$$

so that the pressure from t_k until t_{k+1} is $P_o + P[\tfrac{1}{2}(t_k + t_{k+1}) - t_1]$. The approximation is illustrated in Fig. 5. Note that in the limit $N \to \infty$ ($\Delta t_k \to 0$) the approximation becomes exact. Each interval is chosen such that the response of the system to any of the pressure steps can be treated linearly, i.e. using Eq.(40). Thus at time t_1 (the beginning of the first interval) a pressure $P_1 = p[\tfrac{1}{2}(t_2-t_1)]$ is applied; the structure changes in response to this so that at t_2 (the end of the first interval)

$$\xi(t_2) = \xi_o + \gamma \Delta\xi_1 + (1-\gamma)\, \Delta\xi_1 \{1-\phi[(t_2-t_1)/\tau_1]\}, \qquad (46)$$

where

$$\Delta\xi_1 = (\partial\bar{\xi}/\partial t)_{t_1} \Delta t_1 = (\partial\bar{\xi}/\partial P)_{P_o} (dp/dt)_{t_1} \Delta t_1, \qquad (47)$$

and τ_1 is the structural relaxation time for the thermodynamic and structural conditions appropriate to the t_1 to t_2 interval (the nature of the dependence of τ on the "thermodynamic and structural conditions" is elaborated below). At the beginning of the second interval (time t_2) a second pressure step

$$P_2 = p[\tfrac{1}{2}(t_3+t_2) - t_1] - p[\tfrac{1}{2}(t_2-t_1)]$$

is applied and we must now account for (1) the continuing evolution

of the structure to the first pressure step ΔP_1 except that during the time t_2 to t_3, the relaxation time assumes a new value τ_2 appropriate for the conditions during this second interval; and (2) the response of the system to the pressure change ΔP_2. Thus at time t_3, the time dependent part of the response to ΔP_1 will be given in terms of

$$\phi[(t_2-t_1)/\tau_1 + (t_3-t_2)/\tau_2]$$

and the response to ΔP_2 in terms of

$$\phi[t_3-t_2)/\ \tau_2].$$

The value of ξ at t_3 is therefore

$$\xi(t_3) = \xi_o + \gamma\Delta\xi_1 + (1-\gamma)\Delta\xi_1\{1-\phi[(t_2-t_1)/\tau_1 + (t_3-t_2/\tau_2]\}$$
$$+\gamma\Delta\xi_2 + (1-)\Delta\xi_2\{1-\phi[(t_3-t_2)/\tau_2]\} \qquad (48)$$

where $\Delta\xi_2$ is defined analogously to $\Delta\xi_1$ in Eq. (47).

The form of the general result now becomes clear. At time t (the end of the $N^{\underline{th}}$ interval) we must account for the response to N pressure steps ΔP_1, $\Delta P_2 \ldots \Delta P_N$ imposed at times $t_1, t_2 \ldots t_N$ respectively The relaxation function describing the dynamical part of the response to the $k^{\underline{th}}$ of these pressure changes is

$$\phi[(t_{k+1}-t_k)/\tau_k + (t_{k+2}-t_{k+1})/\tau_{k+1} + \ldots + (t-t_N)/\tau_N]$$

where τ_k is the structural relaxation time for the thermodynamic and structural conditions of the $k^{\underline{th}}$ interval. Therefore we get the result

$$\xi(t)=\xi_o+\gamma\sum_{k=1}^{N}\Delta\xi_k+(1-\gamma)\sum_{k=1}^{N}\Delta\xi_k\{1-\phi[\sum_{j=k}^{N}(t_{j+1}-t_j)/\tau_j] \ . \qquad (49)$$

Taking the limit $N\to\infty, \Delta t_j\to 0 (\Sigma_{j=1}^{N}\Delta t_j = t-t_1)$ and letting $\Delta t_j \to dt"$, $\tau_j \to \tau(t")$ and $\Delta\xi_k \to (\partial\bar{\xi}/\partial t')dt'$ allows us to make the replacements

$$\sum_{k=1}^{N} \rightarrow \int_{t_1}^{t}$$

$$\sum_{j=k}^{N} \rightarrow \int_{t'}^{t}$$

which immediately gives Eq. (42). An equivalent and often more useful form of this equation is obtained if the second equality in Eq. (47) is used to rewrite the $\Delta\xi_k$. Here

$$\xi(t) = \xi_1 + \gamma\int_{t_1}^{t} dt'(\partial\bar{\xi}/\partial P)(dp/dt')$$

$$+(1-\gamma)\int_{t_1}^{t} dt'(\partial\bar{\xi}/\partial P)(dp/dt')\{1-\phi[\int_{t'}^{t} dt''/\tau(t'')]\}. \qquad (50)$$

In order to apply Eq. (42) or (50), it is necessary to specify the nature of the structural ordering parameter ξ, the dependence of τ on P and ξ (and thus on time) and the form of the structural relaxation function $\phi(t/\tau)$. In addition the interplay between the structural and shear relaxation processes must be established. We shall now take up these questions.

B. <u>The Fictive Pressure</u>. Under the isothermal circumstances under consideration here a convenient choice for the ordering parameter describing the structure is the fictive pressure. A material is said to have a fictive pressure P_f if the structure of the material is the structure that would obtain in equilibrium at a pressure $P = P_f$. This definition is analogous to the "fictive temperature" concept introduced and explicated by Tool[4] and Ritland[5] to describe the structural changes in glasses as they are cooled from the melt through their transformation regions.

In the present context the dynamical structure is described at any instant by a time varying fictive pressure $P_f(t)$. The specification of a non-equilibrium state is assumed complete when $P_f(t)$ and the instantaneous pressure $P(t)$ are given. The dynamical behavior of $P_f(t)$ as it evolves toward its equilibrium value $P(t)$ (obviously, from the way it is defined, the equilibrium fictive pressure is just $\bar{P}_f = P$). If a small pressure increase ΔP is imposed at time t_1 on a system previously in equilibrium at pressure P_o, the time variation of $P_f(t)$ is given by an equation of the form of Eq. (40). Specifically, we take:

$\xi(t) = \bar{P}_f(t)$. The structural ordering parameter is the fictive pressure.

$\xi_o = P_o$ and $\xi_\infty = P_o + \Delta P$. The equilibrium value of the fictive pressure is the actual pressure.

$\gamma = 0$. Only relaxational changes in structure are characterized in terms of P_f; any instantaneous changes are presumed to be given explicitly in terms of the change in P.

Thus, Eq. (4) becomes

$$P_f(t) = P_o + \Delta P\{1-\phi[(t-t_1)/\tau]\}. \qquad (51)$$

The response to an arbitrary pressure variation is given by the generalization of the form of Eq. (50):

$$P_f(t) = P_o + \int_{t_1}^{t} dt'(dp/dt')\{1-\phi[\int_{t'}^{t} dt''/\tau(t'')]\} \qquad (52)$$

where we have used the fact that $\partial\bar{P}_f/\partial p = 1$ to simplify the integrand.

In order to evaluate this, the behavior of τ with time must be known. In the spirit of Narayanaswamy and Gardon[6,7] (who deal with isobaric temperature changes) we can deal with this phenomenologically by recognizing that τ depends on both P and P_f. If the structural relaxation time measured as an equilibrium material property, varies with pressure as

$$\tau_{eq} = f(P), \tag{53}$$

then we assume that, for a given non-equilibrium state (characterized by P and P_f), τ is given by

$$\tau = f[xP + (1-x)P_f] \tag{54}$$

where x ($0<x<1$) is a parameter characterizing the relative dependence of the relaxation time on pressure and fictive pressure. We designate it as the "structure coefficient." Now since both P and P_f are time varying we use this in Eq.(52) as

$$\tau(t") = f[xP(t") + (1-x)P_f(t")]. \tag{55}$$

Observe that in order to compute $P_f(t)$ from Eq.(52), it is necessary that $\tau(t")$--and thus $P_f(t")$--be known only for $t_1<t"\leq t$. One can thus proceed in a stepwise fashion to calculate $P_f(t)$ for all $t>t_1$ since, presumably, $\tau(t_1)$ is known as an equilibrium property.

This provides us with a clue for computing the shear stress variation $\sigma(t)$ or equivalently the effective viscosity $\mu(t)$ in the presence of the Hertzian pressure pulse. We examine Eq.(23) or Eq.(24) and regard the shear relaxation function $\phi_s(t")$ as a function of the reduced time variable $t"/\tau_s$. We then assume that τ_s varies in time through the contact zone as a result of the changing pressure and structure in a manner analogous to Eq. (55) for the

strucutral relaxation time; viz.,

$$\tau_s(t") = g[xP(t") + (1-x)\, P_f(t")]. \qquad (56)$$

where the function g(P) gives the pressure variation of the shear relaxation time measured as an equilibrium property. Using this the effective viscosity, for example, would be given by

$$\mu(t) = G_\infty \int_{t_1}^{t} dt' \, \phi_s[\int_{t'}^{t} dt"/\tau_s(t")] \qquad (57)$$

where the generalization of the argument of ϕ_s comes about in essentially the same way that the similar generalization of the argument of ϕ does in Eq. (50). Note that in writing Eq.(57) we have assumed that the variation of G_∞ in the contact zone can be ingored. This is not a necessary restriction; indeed by characterizing the dependence of G_∞ on pressure and structure, the time dependence of G_∞ through the contact could be accounted for. In this paper, however, we shall continue to ignore this variation as the essential features of the stress variation and the tractive force behavior are illustrated rather well without it; at this point including it would seem to be a somewhat uncalled for refinement.

C. The Free Volume. While the computations reported in this paper are carried out using the fictive pressure concept as a means of characterizing the structure, an alternative, and perhaps more familiar approach, makes use of the idea of free volume[8] for describing the structure. The dynamical structure parameter $\xi(t)$ is taken to be the instantaneous free volume

$$v_f(t) = V(t) - V_C \qquad (58)$$

where $V(t)$ is the instantaneous molar volume of the system and V_c is the "close-packed" volume. For a system in equilibrium at a pressure P_o, the time dependence of the structure following the imposition of a small pressure change ΔP at time t_1 is then given by an equation of the form of (40); specifically

$$v_f(t) = v_{fo} + \frac{\kappa_\infty}{\kappa}(v_{f_\infty}-v_{fo}) + (1-\frac{\kappa_\infty}{\kappa})(v_{f_\infty} - v_{fo})\{1-\phi[(t-t_1)/\tau]\}. \quad (59)$$

In this equation v_{fo} and v_{f_∞} are the equilibrium values of the free volume for pressures P_o and $P_o + \Delta P$ respectively, κ_∞/κ (which plays the role of γ) is the ratio of the instantaneous (or glassy) and the equilibrium compressibilities. The generalization of this to obtain the response to an arbitrary pressure change imposed at t_1 is of the form of Eq.(50):

$$v_f(t) = v_{fo} - \kappa_\infty \int_{t_1}^{t} dt'\, v(t')\,(dp/dt')$$

$$-(\kappa_\infty - \kappa_o)\int_{t_1}^{t} dt'\, v(t')\,(dp/dt')\,\{1-\phi[\int_{t'}^{t} dt''/\tau(t'')]\}, \quad (60)$$

where we have assumed that V_c is pressure independent. In order to use this we must relate the time varying shear and structural relaxation times, τ_s and τ respectively, to the free volume. Generally one takes[9]

$$\tau \text{ or } \tau_s \propto \exp(A/v_f)$$

where A is a constant. Using this Eq. (60) provides $v_f(t)$ which can in turn be used to give the time dependence of τ_s. This last is substituted in Eq. (57) to give the effective time dependent viscosity or shear stress.

III DESCRIPTION OF THE CALCULATION

The calculational program presented in the preceeding section has been carried out to determine which of the viscoelastic and material properties are of prime importance in determining the time-dependent shear stress and thus the traction. We consider that the pressure variation through the contact zone is of the Hertzian semi-elliptical form [Eq.(12)]:

$$p(t) = P_{HZ}\,[1-(2t/t_o)^2]^{\frac{1}{2}} \quad (0\leq t\leq t_o). \tag{61}$$

For the maximum Hertzian pressure P_{HZ}, values of 7.5 kbar, 15 kbar, and 30 kbar have been considered. Transit times t_o in the range 10^{-7}s to 10^{-3}s (corresponding to rolling speeds larger than about 80 cm/s for 15 cm diameter steel disks) have been examined.

To describe the instantaneous structure of the lubricant we have used the concept of fictive pressure outlined above. The dependence of the structural and shear relaxation times on the instantaneous state of the system (described by P and P_f) is assumed to be of the form

$$\left(\frac{\tau}{\tau_s}\right) = \left(\frac{\tau}{\tau_{so}}\right) \exp\{\alpha\,[xP + (1-x)P_f]\} \tag{62}$$

where α is the pressure viscosity coefficient (we shall assume that $G_\infty = \eta/\tau_s$ is pressure independent). Observe that in equilibrium ($P_f = P$) this corresponds to the familiar $\eta \propto \exp(\alpha P)$ form for the pressure variation of viscosity.[10] The "zero pressure" shear relaxation time τ_{so} is given in terms of η_o the viscosity at the inlet to the contact zone as

$$\tau_{so} = \eta_o/G_\infty \tag{63}$$

and the ratio of structural to shear relaxation times is assumed to be a pressure independent characteristic parameter for a given substance. Values of x generally fall in the range 0.4 to 0.6.[11-13]

The time evolution of the fictive pressure--given by Eq.(52) with t_1=0--and thus of the relaxation times is governed by the structural relaxation function $\phi(t/\tau)$. The shear stress dynamics, Eq.(57), are determined by the shear relaxation function $\phi_s(t/\tau_s)$. Three forms of these functions, which we distinguish as $\phi^{(1)}(t/\tau)$, $\phi^{(2)}(t/\tau)$ and $\phi^{(3)}(t/\tau)$, were considered in the calculations. The first of these is a simple exponential decay

$$\phi^{(1)}(t/\tau) = \exp(-t/\tau), \tag{64}$$

which we examine in the spirit of a "zeroeth order approximation." A somewhat more realistic form is the so-called fractional exponential decay function

$$\phi^{(2)}(t/\tau)' = \exp[-(t/\tau')^{\beta}] \qquad (0<\beta\leq 1); \tag{65a}$$

the average relaxation time and the decay constant τ' are related by

$$\tau \equiv \int_0^{\infty} dt\,\phi^{(2)}(t/\tau) = (\tau'/\beta)\,\Gamma(1/\beta) \tag{65b}$$

where $\Gamma(\ )$ designates the gamma function. Experimentally this form is found to do a rather good job of describing structural relaxation data in a number of non-polymeric substances with a value of β in the range of roughly 1/3 to 2/3.[14-16] In polymeric liquids the short time part of the response is also fit rather well by the fractional exponential function but for long times ($t>\tau'$), the decay is considerably less rapid; that is, there is a long time

"tail" on the relaxation function.[17-18] To examine the behavior of such materials we consider a third form of the relaxation functions:

$$\phi^{(3)}(t/\tau) = a \exp\left[-(t/\tau)^{\beta}\right] + (1-a) \exp(-t/\tau'') \qquad (66a)$$

where $0<a<1$ and $\tau''>>\tau'$. The average relaxation time for this function is given by

$$\tau = a(\tau'/\beta)\Gamma(1/\beta) + (1-a)\,\tau''. \qquad (66b)$$

The specific functions $\phi^{(2)}$ and $\phi^{(3)}$ examined are characterized by the values $\beta = \frac{1}{2}$, $a = 0.8$ and $\tau''/\tau' = 200$. A comparison of the three functional forms is shown in Figure 6.

Values of the various parameters describing the viscoelastic behavior were chosen in ranges typical of what is commonly found in lubricating fluids. In addition to the three types of relaxation functions we take the following:

Shear Rigidity Modulus = $G_\infty = 2 \times 10^{10}$ dynes/cm^2;

Structure Coefficient = $x = 0.5$

Inlet Viscosity = η_o = 0.1P, 10P, and 10^3P;

Relaxation Time Ratio = τ/τ_s = 1,3, and 10

Pressure Viscosity Coefficient = α = 1 kbar^{-1}, 2 kbar^{-1}, and 4 kbar^{-1}.

The actual calculations of $P_f(t)$ and $\mu(t)$ via Eqs.(52) and (57) was carried out by dividing the time range t=0 to $t=t_Q$ into N=200 subintervals as described in section II.4 above (taking a larger number of subintervals did not significantly alter the results). The intervals were selected according to Eq. (45) such that equal magnitude pressure changes $\Delta P = \pm 2P_{HZ}/N$ occur during

each; the pressure during the $k^{\underline{th}}$ interval ($k<N/2$) is just $k\Delta P$ (P_o being taken as zero). The relaxation times τ and τ_s for each interval were calculated using Eq. (62) in which, for the $k^{\underline{th}}$ interval, for example, P was taken as $k\Delta P$ and P_f was assigned its value at the end of the $(k-1)^{\underline{th}}$, i.e., the preceeding, interval. Thus, for instance, during the first interval $0<t\leq t_2$, the relaxation times are related to their "zero pressure" values τ_o and τ_{so} by the factor $\exp(\alpha x \Delta P)$, the fictive pressure being zero ($=P_o$) at the start of this interval. Using this, Eqs. (52) and (57) can be evaluated straightforwardly to give $P_f(t)$ and $\mu(t)$ for $0\leq t\leq t_2$. For the next interval, the relaxation times are given by the factor $\exp\{\alpha[2x\Delta P + (1-x)P_f(t_2)]\}$ and thus Eqs. (52) and (57) provide $P_f(t)$ and $\mu(t)$ for $t_2<t\leq t_3$. This procedure is iterated until $P_f(t)$ and $\mu(t)$ are mapped out over the entire range $t=0$ to $t=t_o$. It is then a straightforward matter to integrate $\mu(t)$ and thus obtain the tractive force.

IV. RESULTS AND DISCUSSION

1. General Nature of the Results

To illustrate the general features of the calculation on which our attention will be focused, we consider the results of a computation performed for a maximum Hertzian pressure P_{HZ} = 15 kbar and $t_o = 10^{-4}$s (U ≈ 20 m/s). The characteristic liquid properties were taken as:

$G_\infty = 2 \times 10^{10}$ dynes/cm^2;

$\eta_o = 10$ P;

$x = \frac{1}{2}$;

$\alpha = 2$ kbar^{-1};

$\tau/\tau_s = 3$;

$\phi(t/\tau) = \exp(-t/\tau)$

$\phi_s(t/\tau_s) = \exp(-t/\tau_s)$

The computed behavior of $P_f(t)$ and $\mu(t)$ under these circumstances are shown in Figure 7. Consider first the fictive pressure variation. Initially the viscosity and hence the relaxation times are small and the system is able to equilibrate in response to the applied pressure changes. As the pressure becomes larger the relaxation time becomes longer so that the system is no longer able to respond to the changing pressure; the fictive pressure changes relatively little for $t \geq 5 \times 10^{-6}$s. indicating that the structure of the material has been "frozen in." Observe that, from Fig. 8, this transition from viscous liquid to amorphous solid behavior sets in when $\tau \approx 10^{-5}$s, that is, when τ is on the order of the time scale for the occurrence of the significant pressure changes. Further increases in pressure have little effect on the materials' structure; for most of the time that is is in the contact zone, the lubricant behaves as an amorphous solid with a structure that the equilibrium material would have at a pressure of about 4 kbar. Eventually for $t \approx 90 \times 10^{-6}$s, the pressure has fallen to a point where the relaxation times are sufficiently short that the material can again respond to the changing pressure. This is reflected in

the behavior of the fictive pressure as it attempts to equilibrate at the value of the applied pressure.

The time dependent shear stress or effective viscosity also reflects this kind of behavior. Initially ($t <$ a few μs) the shear relaxation time is quite short and the stress is relaxed by viscous flow. However when τ_s becomes relatively long ($t > 10\ \mu s$) the stress increases linearly with time with a slope of G_∞; this is just the behavior of an ideal elastic solid for which

$$\sigma(t) = G_\infty\, \varepsilon(t) = G_\infty t\dot{\varepsilon};\ \ \bar{\mu}(t) = G_\infty t. \tag{67}$$

This behavior is shown by the broken line in Fig. 7.

From Eqs. (27) and (3) the traction coefficient can be written as (for small slip)

$$C_T = \left(\frac{8R}{\pi hE}\right)\ [\bar{\mu}/\tfrac{1}{2}G_\infty t_o]\cdot G_\infty\ \frac{\Delta U}{U} \tag{68}$$

It is apparent from this equation that a large value of the shear rigidity G_∞ leads to large coefficients of traction. It is also clear that (for a given film thickness) the initial slope of the traction curve is determined by the quantity in square brackets. We designate this as χ, the reduced traction slope:

$$\chi = \bar{\mu}/\tfrac{1}{2}G\ t_o. \tag{69}$$

For the situation just described, integrating the $\mu(t)$ curve shown in Fig. 7 leads to $\chi = 0.91$; the initial traction curve slope is 91% of what would be obtained for an elastic solid film of the same thickness. In the following sections we consider the effect on χ of varying P_{HZ}, t_o, η_o, α, τ/τ_s and the forms of ϕ and ϕ_s. In

considering the effect of changing P_{HZ}, t_o, η_o and α we should also consider the variation of the film thickness with these quantities. Empirically[19]

$$h \propto \alpha^{0.6} (\eta_o/t_o)^{0.7} P_{HZ}^{0.45} \tag{70}$$

Consequently we shall also consider the quantity

$$\chi' \equiv (h_o/h)\, \chi \tag{71}$$

where h_o is the film half-thickness for $\alpha = 2$ kbar^{-1}, $\eta_o = 10$ P, $P_{HZ} = 15$ kbar, and $t_o = 10^{-4}$s.

2. Effect of Varying the Rolling Speed and the Maximum Hertzian Pressure

The time variation of the fictive pressure and shear stress were computed for maximum Hertzian pressures of 7.5 kbar for several values of the transit time t_o. The reduced traction slopes χ (as well as the values of χ') were obtained from these. The lubricant parameters were taken as $\alpha = 2$ kbar^{-1}, $\eta_o = 10$ P and $\tau/\tau_s = 3$. The fractional exponential from of the relaxation functions, e.g., $\phi(t/\tau) = \exp[-(t/\tau)^{\beta}]$, with $\beta = 0.5$ was assumed. The results are presented in Figs.9 and 10 and in Table I. The general behavior is quite similar to what was noted above. The fictive pressure first rises rapidly in response to the impressed pressure change, then levels off when the structural relaxation time becomes long and ultimately drops precipitously when the pressure is reduced as the lubricant leaves the contact zone. For most of the transit time the structure (the fictive pressure) is unchanging and can be characterized by the maximum value $P_{f,max}$.

Observe that as the transit time is decreased (rolling speed increased) the value of $P_{f,max}$ decreases for a given value of P_{HZ}. This is to be expected since for small transit times the ability of the material to equilibrate with the changing pressure is inhibited.

Note also that for a given value of t_o, increasing P_{HZ} causes a <u>decrease</u> in $P_{f,max}$. This result, surprising at first, can be understood in much the same sort of way. Increasing P_{HZ} (for fixed t_o) also increases the <u>rate</u> at which the pressure is changing and consequently reduces the ability of the structure to remain in equilibrium. The effect of either increasing the Hertzian pressure or decreasing the transit time is to cause the lubricant to act in a solid-like fashion for a larger fraction of the time that it spends in the contact. This is evident in the behavior of the shear stress or time dependent viscosity $\mu(t)$ and is reflected in the variation of χ with both t_o and P_{HZ}. At the highest pressure one finds essentially elastic solid behavior whereas at 7.5 kbar, the value of χ varies from about one-quarter to one-half of what would be found in a solid. It is interesting to observe that if one were to interpret the corresponding traction curve slopes as the shear modulus G_∞ (effectively putting $\chi = 1$), one could infer as much as a four-fold increase in G_∞ as P_{HZ} increases from 7.5 kbar to 30 kbar. This is, or course, entirely spurious as we have taken G_∞ to be constant (2×10^{10} dynes/cm^2).

3. Effect of Varying the Pressure-Viscosity Coefficient

To examine the effect on traction of different values of the pressure, we have performed the calculations for the situations outlined below:

External Variables: P_{HZ} = 15 kbar

t_o = 100 μs (U=20 m/s);

Lubricant Properties: $G_\infty = 2 \times 10^{10}$ dynes/cm^2,

η_o = 10 P,

τ/τ_s = 3,

$\phi = \exp\,[-(t/\tau')\cdot^5]$,

$\phi_s = \exp\,[-(t/\tau_s')\cdot^5]$,

and

α = 1 kbar^{-1}, 2 kbar^{-1}, 4 kbar^{-1}.

The time dependent quantities $P_f(t)$ and $\mu(t)$ are shown in Figure 11 for these circumstances. A summary of the results is given in Table II. From these it is apparent that increasing α has an effect quite similar to increasing P_{HZ}. This is not surprising as α and P appear in the calculation as a product in the formula for the pressure dependence of τ and τ_s; consequently their influence on the traction curves is symmetric.

4. Effect of Varying the Inlet Viscosity

For the situation described by the external variables

P_{HZ} = 15 kbar,

t_o = 100 μs (U = 20 m/s)

and η_o = 0.1P, 10 P and 10^3 P,

the results are shown in Figure 12 and Table III. As is apparent, a higher inlet viscosity--corresponding to longer relaxation times at the entrance to the contact--limits the ability of the lubricant to adjust its structure to the pressure changes in the contact and, as a result, causes it to behave in a glassy fashion for a larger fraction of the transit time. Observe, from the X' variation, that the major effect is associated with changes in the film thickness.

4. Effect of Varying the Relaxation Time Ratio τ/τ_s

For the same external conditions as were considered above and for the liquid properties as above (with η_o = 10 P) we consider the changes that result from allowing τ/τ_s to take on the values 1,3 and 10. As is evident from the results given in Table IV, the effects on the traction parameters χ and χ' are quite small. The decrease in $P_{f,max}$ as τ/τ_s is increased is traceable to the larger values of τ at the inlet (τ_s at the inlet is the same in all cases); consequently the solid-like behavior sets in somewhat earlier for larger values of τ/τ_s.

5. Effect of Changing the Form of the Relaxation Functions

To examine the importance of the detailed shape of the relaxation functions $\phi(t/\tau)$ and $\phi_s(t/\tau_s)$ in determining the lubricant behavior in an EHD contact, we have examined four separate cases:

Case I: $\phi(t/\tau) = \phi^{(1)}(t/\tau)$,

$\phi_s(t/\tau_s) = \phi^{(1)}(t/\tau_s)$;

$$\text{Case II:} \quad \phi(t/\tau) = \phi^{(2)}(t/\tau)$$
$$\phi_s(t/\tau_s) = \phi^{(2)}(t/\tau_s);$$

$$\text{Case III:} \quad \phi(t/\tau) = \phi^{(2)}(t/\tau)$$
$$\phi_s(t/\tau_s) = \phi^{(3)}(t/\tau_s);$$

$$\text{Case IV:} \quad \phi(t/\tau) = \phi^{(3)}(t/\tau)$$
$$\phi_s(t/\tau_s) = \phi^{(3)}(t/\tau_s).$$

The functions $\phi^{(1)}$, $\phi^{(2)}$ and $\phi^{(3)}$ are defined in Eqs. (64) -(66) and have been plotted in Fig. 6. For these functions we have taken $\beta = \frac{1}{2}$, $a = 0.8$ and $\tau'' = 200\ \tau'$. For each of the four cases, we compute $P_f(t)$, $\mu(t)$, χ and χ' for the following conditions:

External Variables: $P_{HZ} = 7.5$ kbar,
$t_o = 100\ \mu s$ ($U = 20$ m/s);

Lubricant Properties: $G_\infty = 2 \times 10^{10}$ dynes/cm^2
$\eta_o = 10$ P
$\alpha = 2$ kbar^{-1}
$\tau/\tau_s = 3$

The results are shown in Figure 13 and Table V.

We consider first the behavior of the fictive pressure. It is clear from the results that for relaxation functions characterized by the same average relaxation time τ (equal viscosities here since G_∞ and τ/τ_s are the same), there is a rather marked difference in the behavior of the fictive pressure. This stems primarily from the enhancement of the short time response materials characterized by a structural relaxation function of the $\phi^{(3)}$ type as compared with those characterized by $\phi^{(2)}$ (which, in the same way allows for more short-

time response than $\phi^{(1)}$). The effect of this short time response capability can be understood by thinking of the relaxation functions as superpositions of exponential decays of the form

$$\sum_i g_i \exp(-t/\tau_i), \tag{72}$$

where the g_i are weighting factors. Suppose for definiteness we take τ (the average relaxation time) = τ_o, i.e. the i=0 term in the sum, and let i run from-M to +M, with $\tau_i < \tau_{i+1}$.

For the simple exponential decay function only $g_o \neq 0$ and we may think of the structure as responding on a time scale τ_o. When the pressure changes occur on a scale long compared with τ_o the structure is able to remain in equilibrium. However when τ_o increases (because of the pressure increase) to a value comparable with the time scale of pressure changes (for the case here when $\tau_o \approx 10^{-5}$s), the material is no longer able to adjust its structure and consequently P_f departs from P.

For the functions $\phi^{(2)}$ and $\phi^{(3)}$ however, all the g_i are non-zero; in particular there are short relaxation time ($\tau_i<\tau$) contributions to the structural relaxation function--the i<0 terms in (72). Consequently even when $\tau_o \approx 10^{-5}$s, there are still structural relaxation processes that are able to respond and as a result there is a continuing (albeit incomplete) evolution of the structure. This is particularly evident in the fictive pressure curves II, III and IV in Fig.13a.

The influence of the short relaxation time contributions on the shear stress (effective viscosity) behavior is somewhat different. The specific nature of the difference can be understood most easily by comparing the curves II and III in Figure 13b. For these, the

structural relaxation (but not the shear relaxation) dynamics are the same. As is evident the shear stress is significantly less (leading to smaller traction slopes) when the short time shear relaxation processes are enhanced. Simply stated this means that even when those contributions to the stress described by long relaxation times are kinetically arrested and are thus behaving in a solid-like manner (again we are thinking of representing ϕ_s as a weighted sum of exponential decays), there are still stress components with short relaxation times present that can be relaxed in a liquid-like fashion. This partial stress relaxation produces the lower stress values and smaller traction slopes for the case $\phi_s = \phi^{(3)}$.

V. SUMMARY

The influence of various liquid lubricant properties on the slope of the traction curves in the low slip/roll region has been evaluated. This slope, given by an expression of the form

$$(8R/\pi hE)\ \chi\ G_\infty,$$

is quite sensitive to certain of these properties and relatively insensitive to others. The effects of each are summarized below.

1. Hertzian Pressure: Increasing P_{HZ} causes χ to approach unity and (for a given rolling speed) causes the film thickness h to decrease; the traction slope therefore increases. If the transit time t_o is fixed, increasing P_{HZ} causes b to increase. Since this increases U, h is increased and this change opposes the change in χ.

2. Rolling Speed: Increasing U causes χ to approach unity and produces an increase in h. For relatively low values of P_{HZ} the former

effect dominates and the traction slope increases; however, when P_{HZ} is sufficiently high that $\chi \approx 1$, the latter effect assumes the major role and causes a reduction in the traction slope with increasing U.

3. Shear Ridigity: As is evident an increase in G_∞ will cause an increase in the traction slope. This is the single most important factor although the practical range of G_∞ values that are available is rather limited.

4. Pressure-Viscosity Coefficient: Increasing α causes χ to increase toward unity but also produces an increase in h. At lower values of P_{HZ}, the increase in χ predominates and this the traction slope increases; when P_{HZ} is high, $\chi \approx 1$ and the increase in h causes the slope to decrease.

5. Inlet Viscosity: Increasing η_o produces essentially the same changes as increasing α. However, since rather large ranges of η_o values are available, the film thickness increase is of greater importance.

6. Relaxation Time Ratio τ/τ_s: Increasing τ/τ_s causes a decrease in χ and in the traction slope. For the ranges of τ/τ_s generally encountered this effect is quite small.

7. Form of the Structural Relaxation Function: Increasing the short time response region of the function $\phi(t/\tau)$ leads to small increases in χ and thus in the slope. If G_∞ had been allowed to vary through the contact region (rather than being held constant), this increase would have been more pronounced as higher fictive pressure values and thus higher shear moduli are achieved when a short-time portion of $\phi(t/\tau)$ is present.

8. Form of the Shear Relaxation Function: Increasing the short relaxation time poriton of $\phi_s(t/\tau_s)$ leads to a decrease in χ and therefore to a decrease in the traction slope.

The liquid properties of chief significance in producing a large reduced traction slope χ are therefore a large shear rigidity, relatively large values of the inlet viscosity and pressure-viscosity coefficient, a structural relaxation function with an enhanced short time response nature and a shear relaxation function without short time response characteristics.

The influence of a pressure and structure dependent shear rigidity and the possibility of extending the calculation into the non-linear region (which is of greater practical significance) of large $\Delta U/U$ values are presently under investigation.

REFERENCES

1. This form is used only for the sake of simplicity; more refined functional relationships can be employed.

2. As with the form for the pressure distribution, this simplified approximation is adequate for the aims of this paper.

3. See, e.g. R. Kubo, J. Phys. Soc. Japan 12, 570 (1957); also L.D. Landan and E.M. Lifshitz, Statistical Physics (Addison Wesley, Reading, Mass. 1958), Chap. 12.

4. A.Q. Tool, J. Amer. Ceram. Soc. 29, 240 (1946).

5. H.N. Ritland, J. Amer. Ceram. Soc. 39, 403 (1956).

6. R. Gardon and O.S. Narayanaswamy, J. Amer. Ceram. Soc. 53, 380 (1970).

7. O.S. Narayanaswamy, J. Amer.Ceram. Soc. 54, 491 (1971).

8. This approach to EHDL problems was used by E.G. Trachman and H.S. Cheng, Report No. NASA CR-2206(NASA Contract No. NGL 14-007-084), March 1973, and by G. Harrison and E.G. Trachman, J. Lub. Tech, Trans. ASME F94, 306 (1972). Our approach differs from their primarily in the treatment of the shear stress relaxation dynamics.

9. A.K. Doolittle, J. Appl. Phys. 22, 1471 (1951).

10. This is an oversimplification but is used here as it forms a "not unreasonable" approximation for most lubricants.

11. C.T. Moynihan et al., J. Amer. Ceram. Soc. 59, 137 (1976).

12. M.A. DeBolt et al., J. Amer. Ceram. Soc. 59, 16 (1976).

13. C.T. Moynihan et al., Ann. N.Y. Acad. Sci. 279, 15 (1976).

14. J. F. Dill, P.W. Drake and T.A. Litovitz, Amer. Soc. Lub. Engr. Trans. 18, 202 (1975).

15. J. A. Bucaro, H.D. Dardy and R.D. Corsero, J. Appl. Phys. 46, 741 (1975).

16. C.C. Lai, P.B. Macedo and C.J. Montrose, J. Amer. Ceram. Soc. 58, 120 (1975).

17. W. Philipoff, "Relaxations in Polymer Solutions, Liquids and Gels" in Physical Acoustics, Vol. IIB, ed. W.P. Mason (Academic Press, New York, 1965).

18. A.J. Barlow et al., Proc. Roy. Soc. A309, 497 (1969) and references cited therein.

19. D. Dowson and G.R. Higginson, Elastohydrodynamic Lubrication. (Pergamon Press, New York, 1966).

TABLE I. The effect of changing the rolling speed and the maximum Hertzian pressure[a].

t_o(μs)	U(m/s)	$P_{f,max}$(kbar)	χ	χ'
P_{HZ} = 7.5 kbar				
10	100	4.33	0.523	0.143
40	25	5.04	0.420	0.320
50	20	5.15	0.402	0.338
66.7	15	5.29	0.381	0.392
100	10	5.48	0.349	0.477
200	5	5.80	0.297	0.659
400	2.5	6.10	0.245	0.883
P_{HZ} = 15 kbar				
10	200	3.56	0.900	0.180
80	25	4.75	0.851	0.728
100	20	4.87	0.845	0.845
133	15	5.03	0.835	1.019
200	10	5.26	0.825	1.340
400	5	5.65	0.805	2.124
P_{HZ} = 30 kbar				
10	400	2.74	.996	0.146
100	40	4.04	.984	0.720

(a) Liquid parameters taken as $G_\infty = 2 \times 10^{10}$ dynes/cm^2, η_o = 10 P, $\tau/\tau_s = 3$, $\alpha = 2$ kbar^{-1}. Relaxation functions are given by Eq. (65) with $\beta = .5$.

TABLE II. Effect of changing the pressure-viscosity coefficient.[a]

α (kbar^{-1})	$P_{f,max}$	χ	χ'
1	10.97	.349	.529
2	4.87	.845	.845
4	2.02	.984	.649

[a] Calculations for P_{HZ} = 15 kbar, $t_o = 10^{-4}$ s, $G_\infty = 2 \times 10^{10}$ dyne/cm^2, η_o = 10 P, τ/τ_s = 3, and relaxation functions given by Eq. (65) with β = .5.

TABLE III. Effect of changing the Inlet Viscosity.[a]

η_o (P)	$P_{f,max}$ (kbar)	X	X'
0.1	7.42	.694	17.4
10	4.87	.845	0.845
10^3	2.26	.942	0.038

[a] $\alpha = 2$ kbar^{-1}, η_o variable; other parameters as in Table II.

TABLE IV. Effect of changing the relaxation time ration τ/τ_s.[a]

τ/τ_s	$P_{f,max}$ (kbar)	χ	χ'
1	5.48	.868	.868
3	4.87	.845	.845
10	4.19	.812	.812

[a] η_o = 10 P, τ/τ_s variable; other parameters as in Table III.

TABLE V. The effect of changing the form of the relaxation function ϕ and ϕ_s.

ϕ and ϕ_s [b]	$P_{f,max}$ (kbar)	χ	χ'	
$\phi = \phi^{(1)}(t/\tau)$ $\phi_s = \phi^{(1)}(t/\tau_s)$	5.14	.444	.607	Case I
$\phi = \phi^{(2)}(t/\tau)$ $\phi_s = \phi^{(2)}(t/\tau_s)$	5.48	.349	.477	Case II
$\phi = \phi^{(2)}(t/\tau)$ $\phi_s = \phi^{(3)}(t/\tau_s)$	5.48	.194	.265	Case III
$\phi = \phi^{(3)}(t/\tau)$ $\phi_s = \phi^{(3)}(t/\tau_s)$	6.18	.225	.307	Case IV

[a] External variables: $P_{HZ} = 7.5$ kbar, $t_o = 10^{-4}$s; liquid properties: $\eta_o = 10$ P, $\alpha = 2$ kbar^{-1}, $\tau/\tau_s = 3$.

[b] $\phi^{(1)}$, $\phi^{(2)}$ and $\phi^{(3)}$ are defined in Eqs. (64)-(66); we have taken $\beta = .5$, $a = .8$ and $\tau'' = 200\ \tau'$.

LIST OF FIGURE CAPTIONS

Figure 1. Twin-disk apparatus for traction measurements.

Figure 2. EHD contact zone geometry.

Figure 3. Typical traction curves measured on a twin-disk apparatus for two maximum Hertzian pressures [Data from K.L.Johnson and R. Cameron, Proc. Inst. Mech. Engrs. (1967-68), 182 Pt. 1, 307.]

Figure 4. (a) A presssure step ΔP applied at time t_1. (b) The response of the structure to that pressure step.

Figure 5. The "series-of-steps" approximation (solid curve) to a smooth pressure variation (dash-dot curve).

Figure 6. The relaxation function $\phi^{(1)}$, $\phi^{(2)}$ and $\phi^{(3)}$, defined in Eqs. (64) - (66), plotted versus reduced time.

Figure 7. Response of a system under the conditions: P_{HZ} = 15 kbar, t_o = 100μs, η_o = 10P, α = 2 kbar^{-1}, τ/τ_s = 3, and $\phi(t/\tau) = \exp(-t/\tau)$. (a) The pressure P (broken curve) and fictive pressure Pf (solid curve) versus time. (b) The effective viscosity or reduced shear stress versus time (solid curve). The behavior of an ideal elastic solid is shown (broken curve) for comparison. The arrow at the left indicates the average effective viscosity $\bar{\mu}$.

Figure 8. The time variation of the structural and shear relaxation times (τ and τ_s respectively) for the same conditions as listed in Fig. 7.

Figure 9. The effect on the structural and shear response of varying the transit time t_o (t_o values shown at the right of the graphs). (a) Pressure (broken curve) and fictive pressure (solid curves) versus t/t_o. (b) Normalized effective viscosity or shear stress versus t/t_o (solid curves); elastic solid behavior (broken curve) is shown for comparison. The arrows at the left indicate the average effective viscosity. For these curves P_{HZ}=7.5 kbar, η_o = 10P, α = 2 kbar^{-1}, τ/τ_s = 3 and ϕ and ϕ_s are given by Eq. (65).

Figure 10. The effect on the structural and shear response of varying the peak Hertzian pressure P_{HZ} (P_{HZ} values shown at the right of the graphs). (a) Fictive pressure versus time. (b) Effective viscosity versus time (solid curves); elastic solid behavior (broken curve) is shown for comparison. The arrows at the left indicate the average effective viscosity. For these curves the conditions are as in Fig. 9, except that t_o = 100 μs and P_{HZ} takes on the values shown.

Figure 11. The effect on the structural and shear response of varying the pressure-viscosity coefficient α (α values shown at the right of the graphs). (a) Fictive pressure versus time. (b) Effective viscosity versus time (solid curves); elastic solid behavior (broken curve) is shown for comparison. The arrows at the left indicate the average effective viscosity. For these curves the conditions are as in Fig. 10 except that P_{HZ} = 15 kbar and α takes on the values shown.

Figure 12. The effect on the structural and shear response of varying the inlet viscosity η_o (η_o values shown at the right of the graphs). (a) Fictive pressure versus time. (b) Effective viscosity versus time (solid curves); elastic solid behavior (broken curve) is shown for comparison. The arrows at the left indicate the average effective viscosity. For these curves the conditions are as in Fig. 11, except that α = 2 $kbar^{-1}$ and η_o takes on the values shown.

Figure 13. The effect of different structural and shear relaxation behavior on the response of the system. The four cases shown are tabulated at the beginning of Section IV-5. (a) Fictive pressure versus time. (b) Effective viscosity versus time (solid curves); elastic solid behavior (broken curve) is shown for comparison. The arrows at the left indicate the average effective viscosity. For these curves the conditions are as in Fig. 12 except that P_{HZ} = 7.5 kbar, η_o = 10P and ϕ and ϕ_s take on the forms indicated.

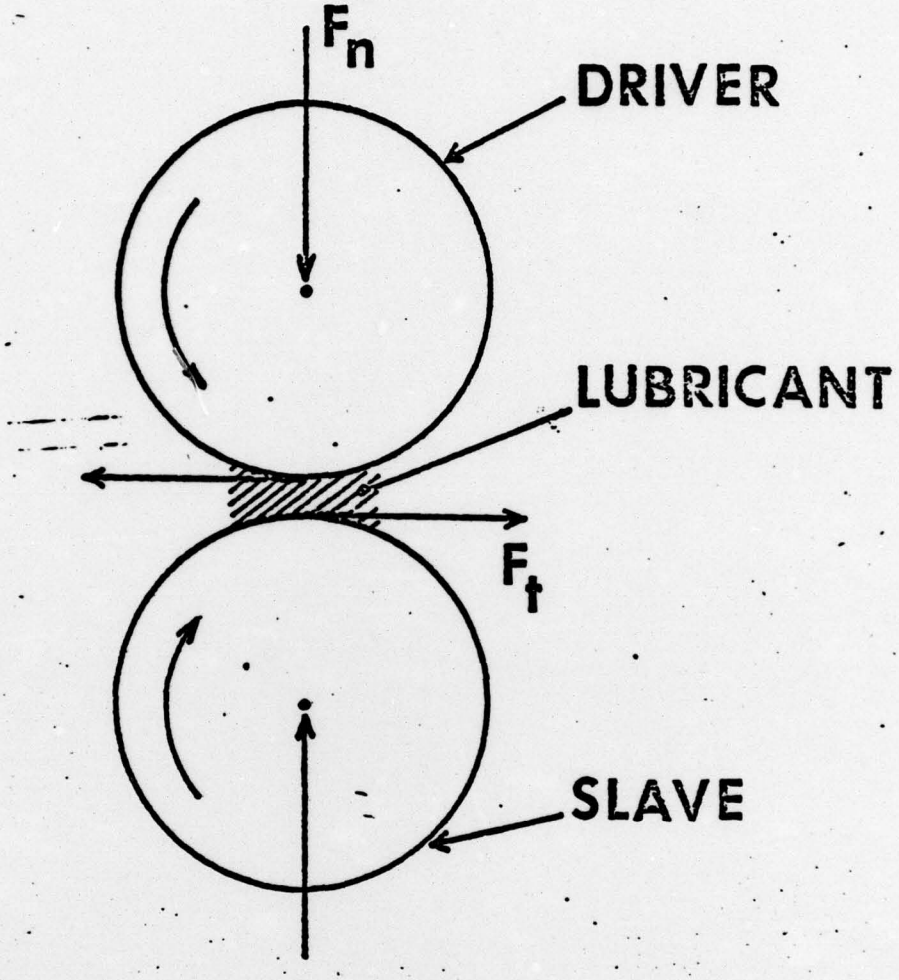

FIGURE 1

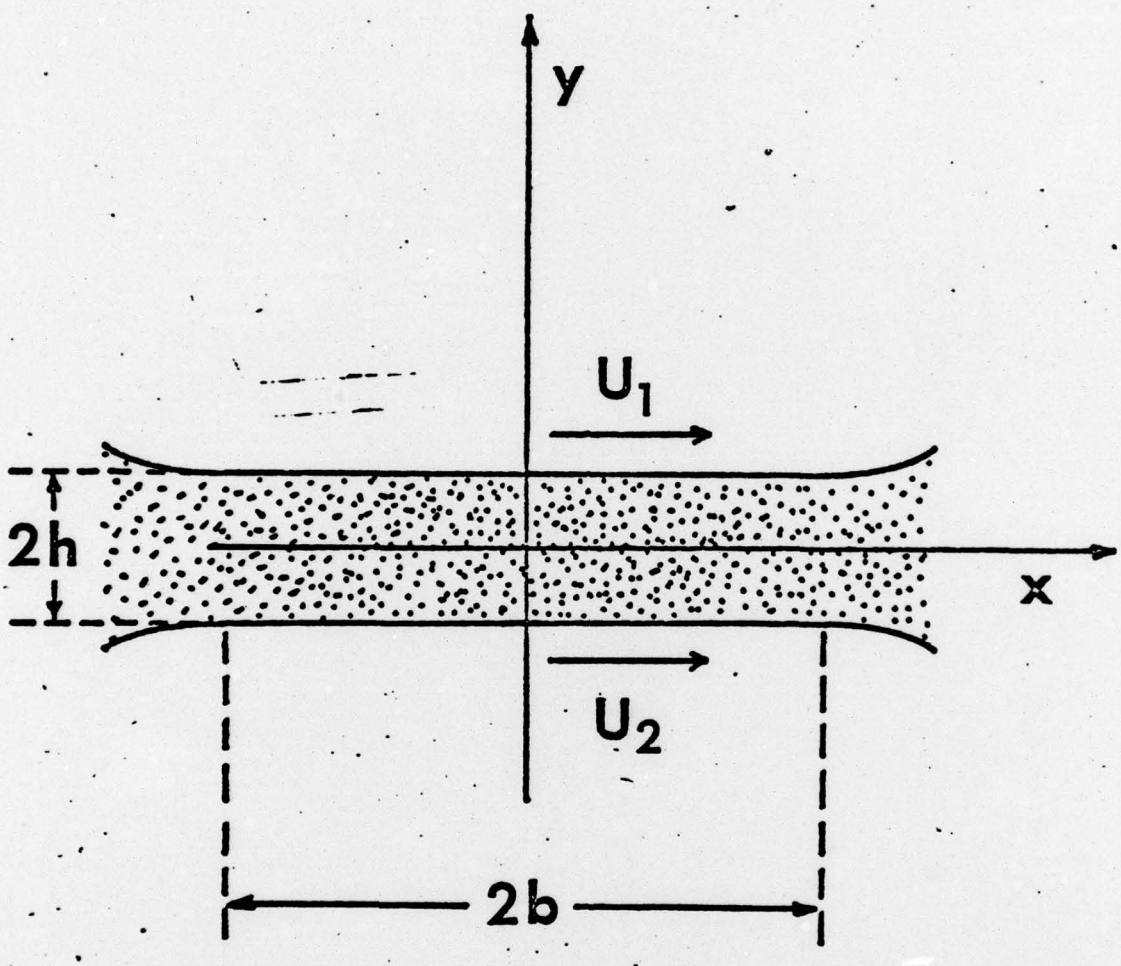

FIGURE 2

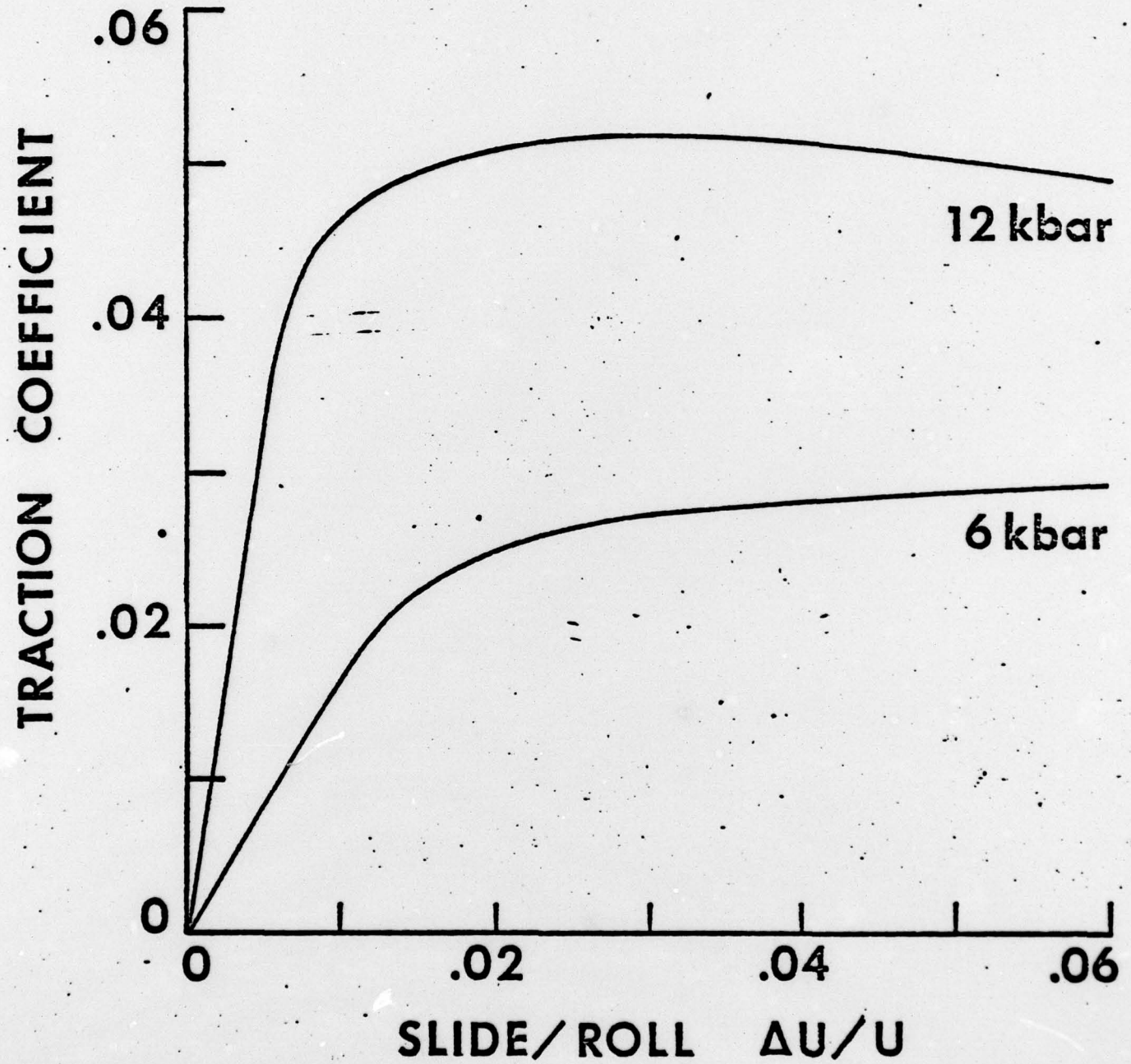
TRACTION COEFFICIENT
.06
.04
.02
0
12 kbar
6 kbar
0
.02
.04
.06
SLIDE/ROLL ΔU/U

FIGURE 3

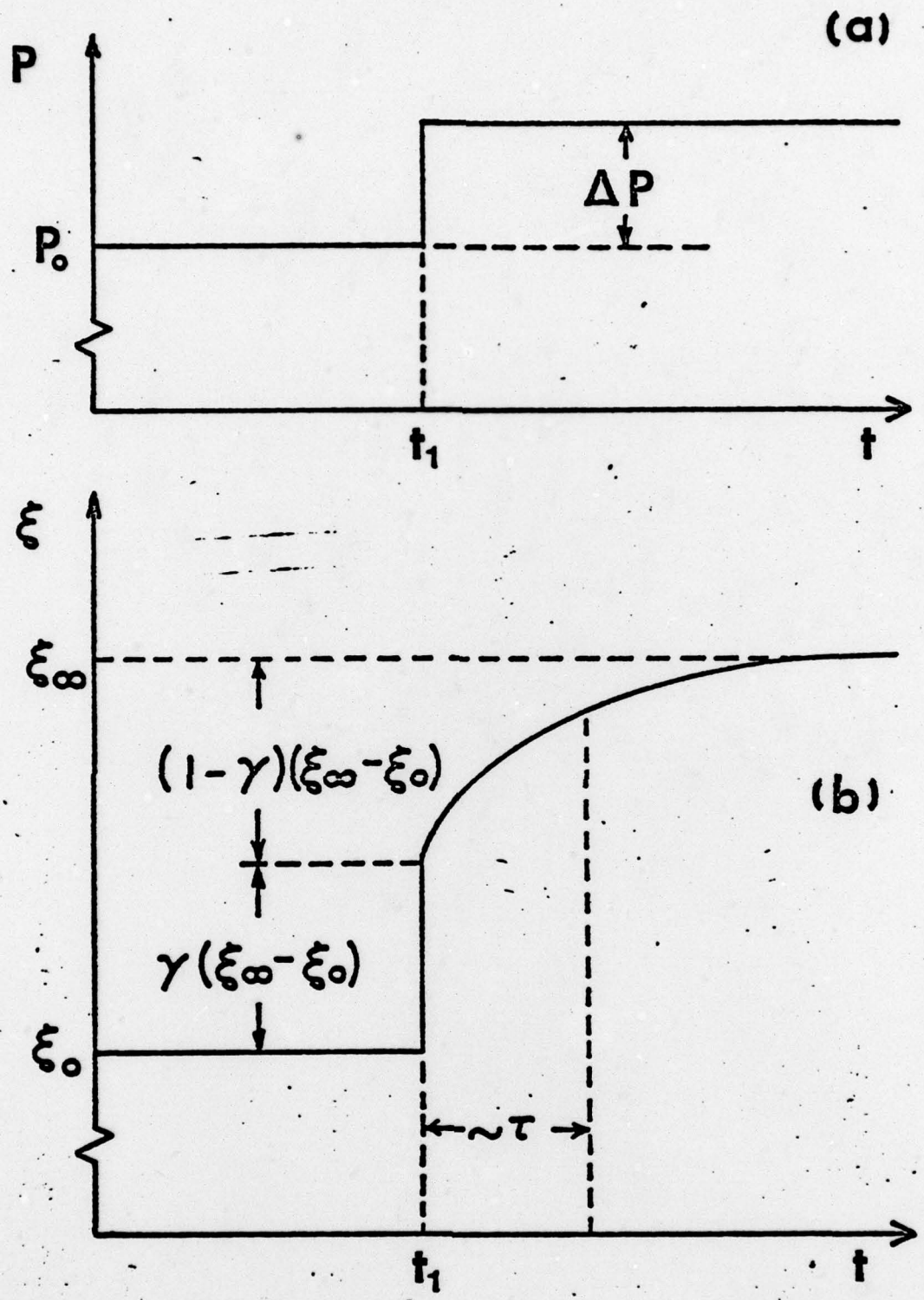

FIGURE 4

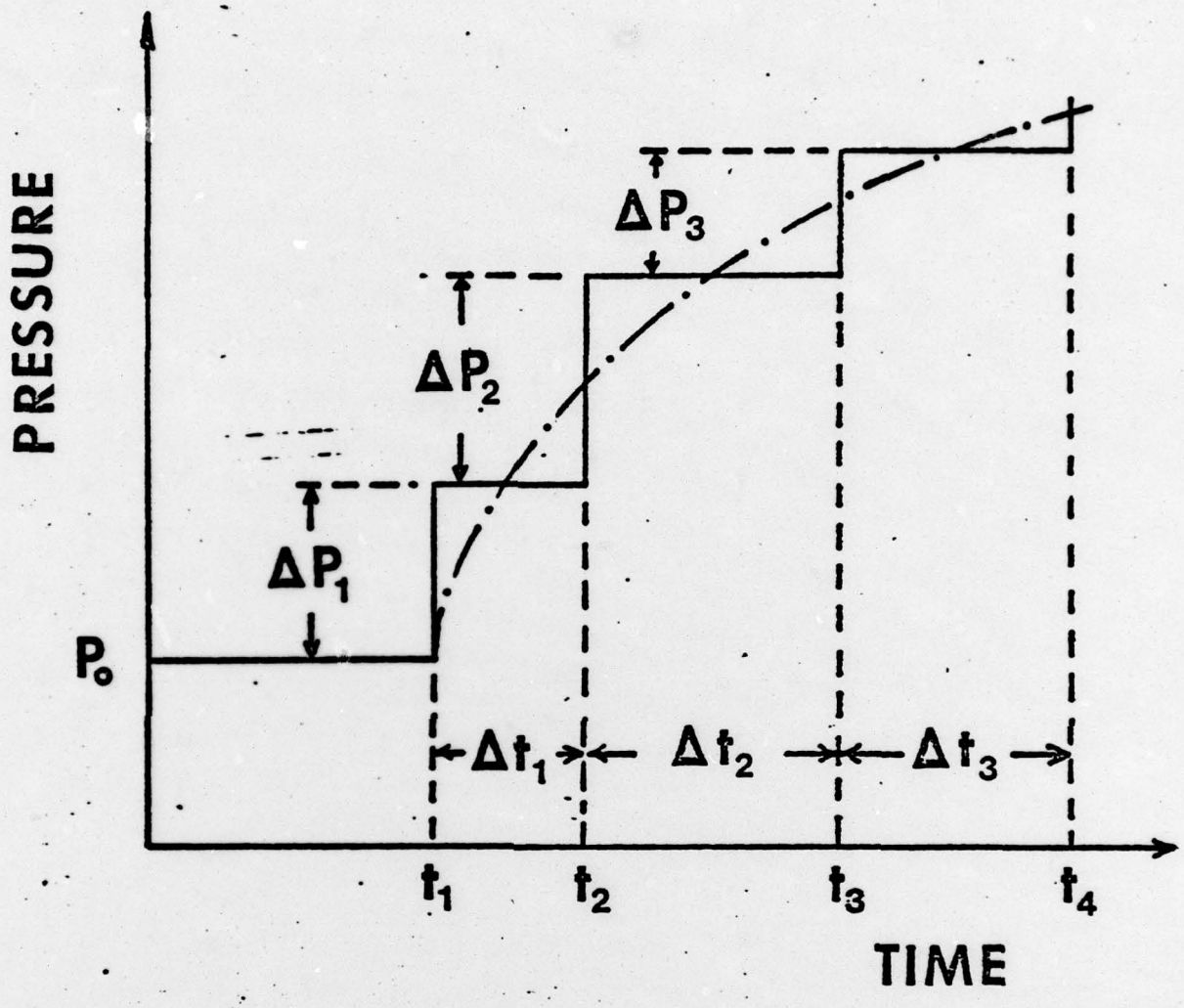
PRESSURE
ΔP_3
ΔP_2
ΔP_1
P_o
Δt_1
Δt_2
Δt_3
t_1
t_2
t_3
t_4
TIME

FIGURE 5

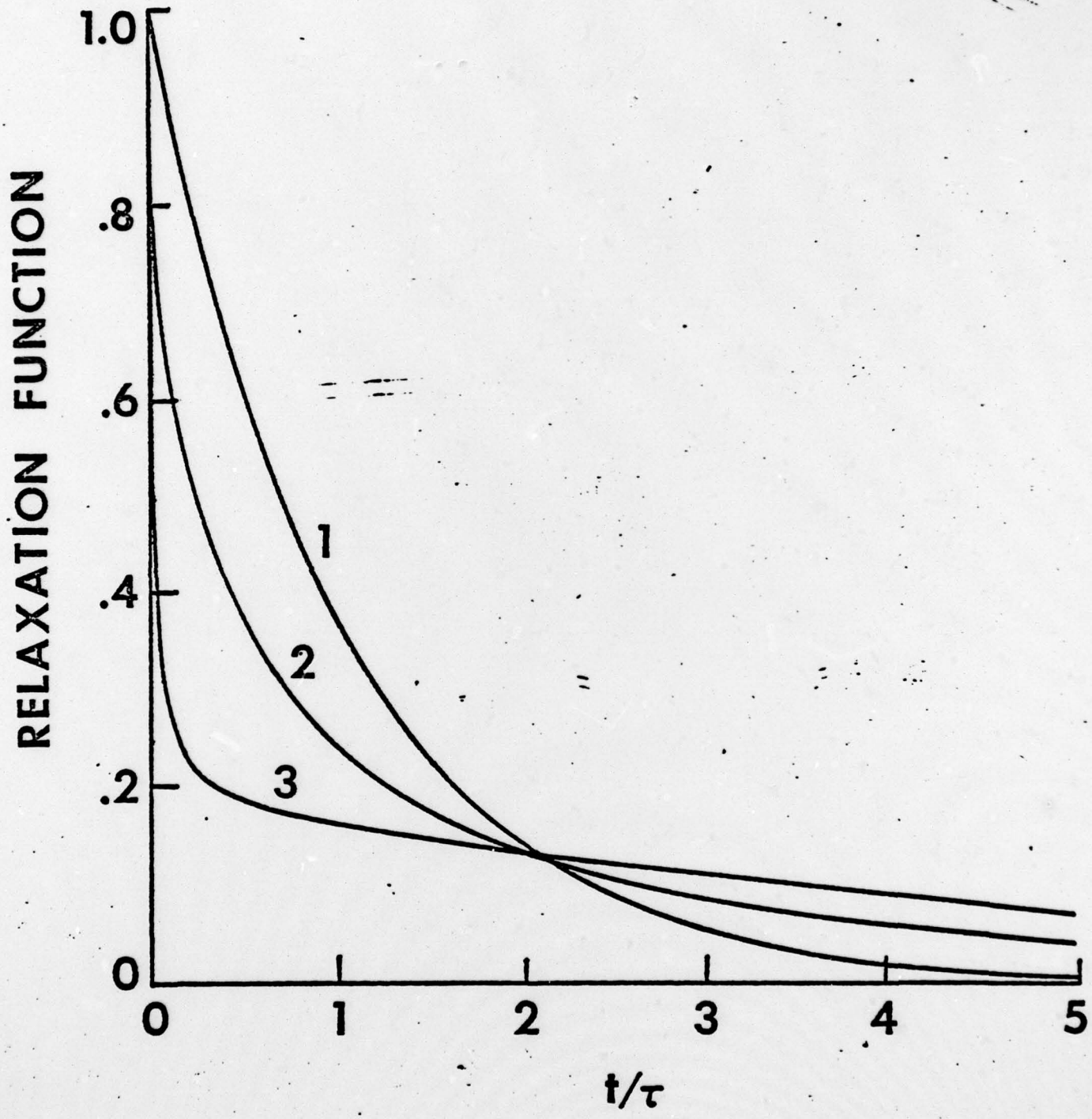

FIGURE 6

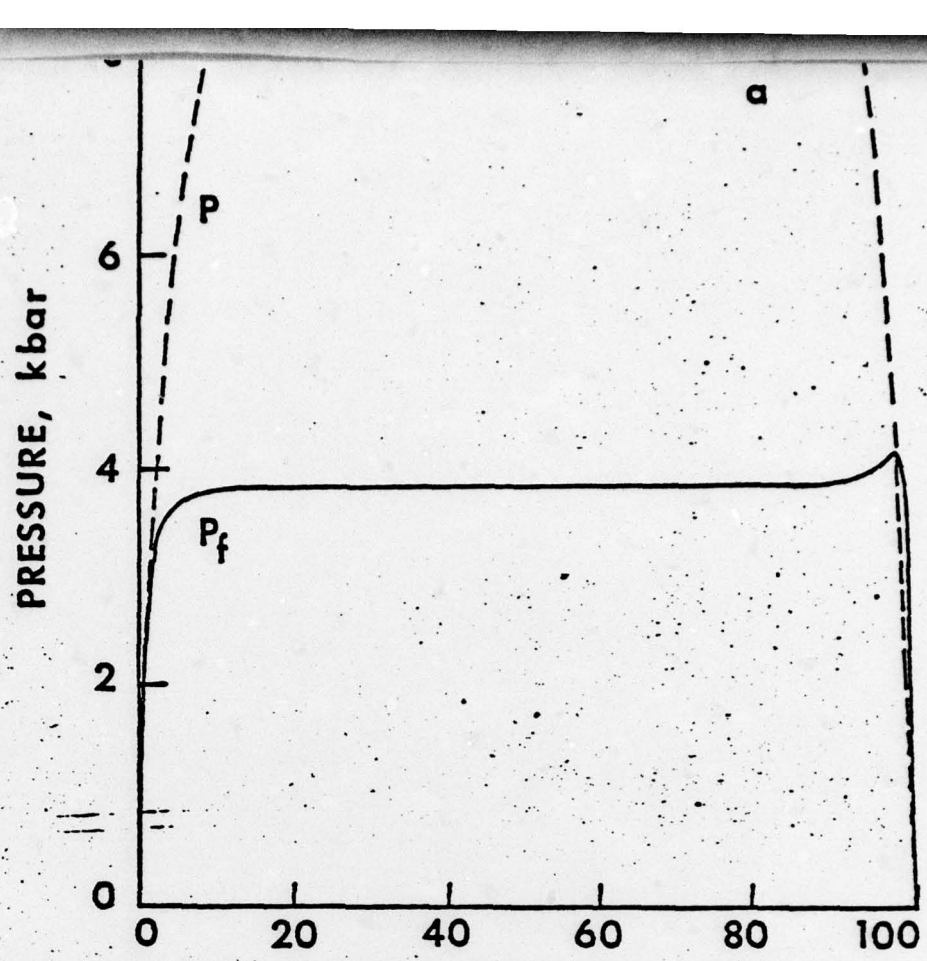
a
P
P_f
PRESSURE, kbar
0
2
4
6
0
20
40
60
80
100

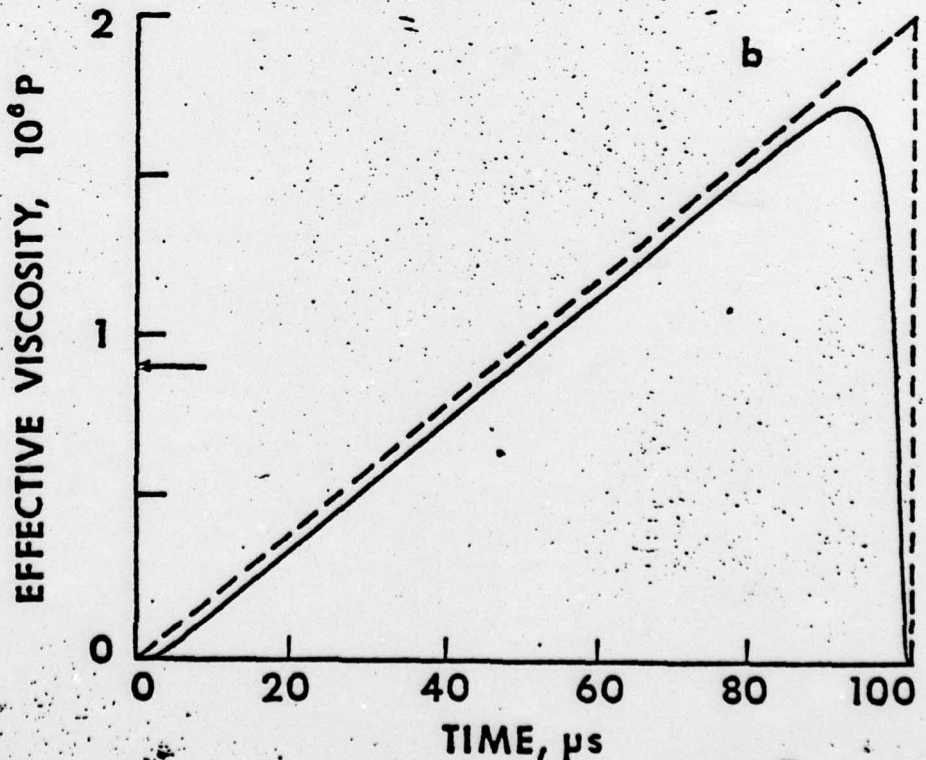
b
EFFECTIVE VISCOSITY, 10^6 P
0
1
2
0
20
40
60
80
100
TIME, μs

FIGURE 7

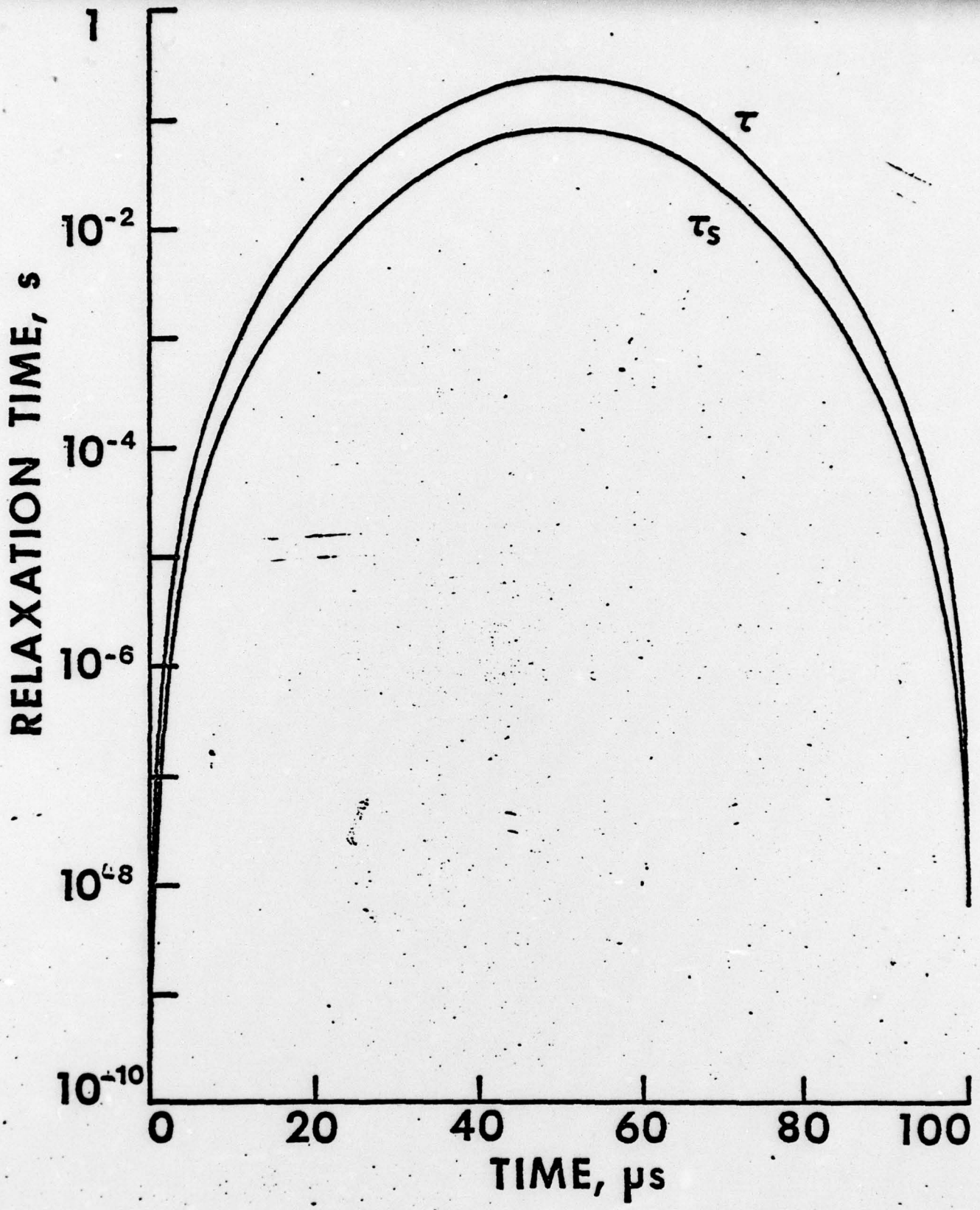
1
10^{-2}
10^{-4}
10^{-6}
10^{-8}
10^{-10}
RELAXATION TIME, s
τ
τ_s
0
20
40
60
80
100
TIME, μs

FIGURE 8

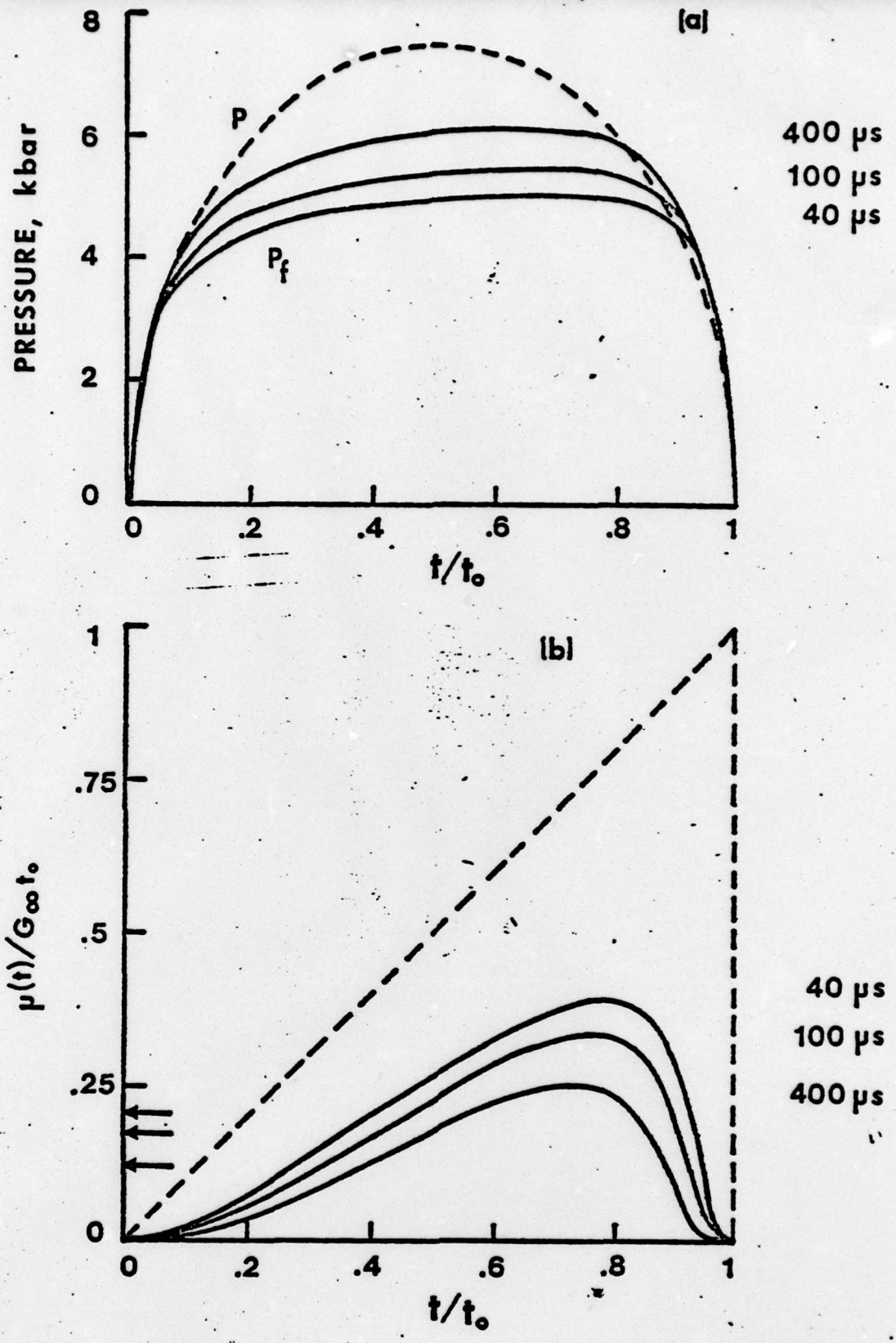
(a)
PRESSURE, kbar
8
6
4
2
0
P
P_f
400 μs
100 μs
40 μs
0
.2
.4
.6
.8
1
t/t_o
(b)
$\mu(t)/G_\infty t_o$
1
.75
.5
.25
0
40 μs
100 μs
400 μs
0
.2
.4
.6
.8
1
t/t_o

FIGURE 9

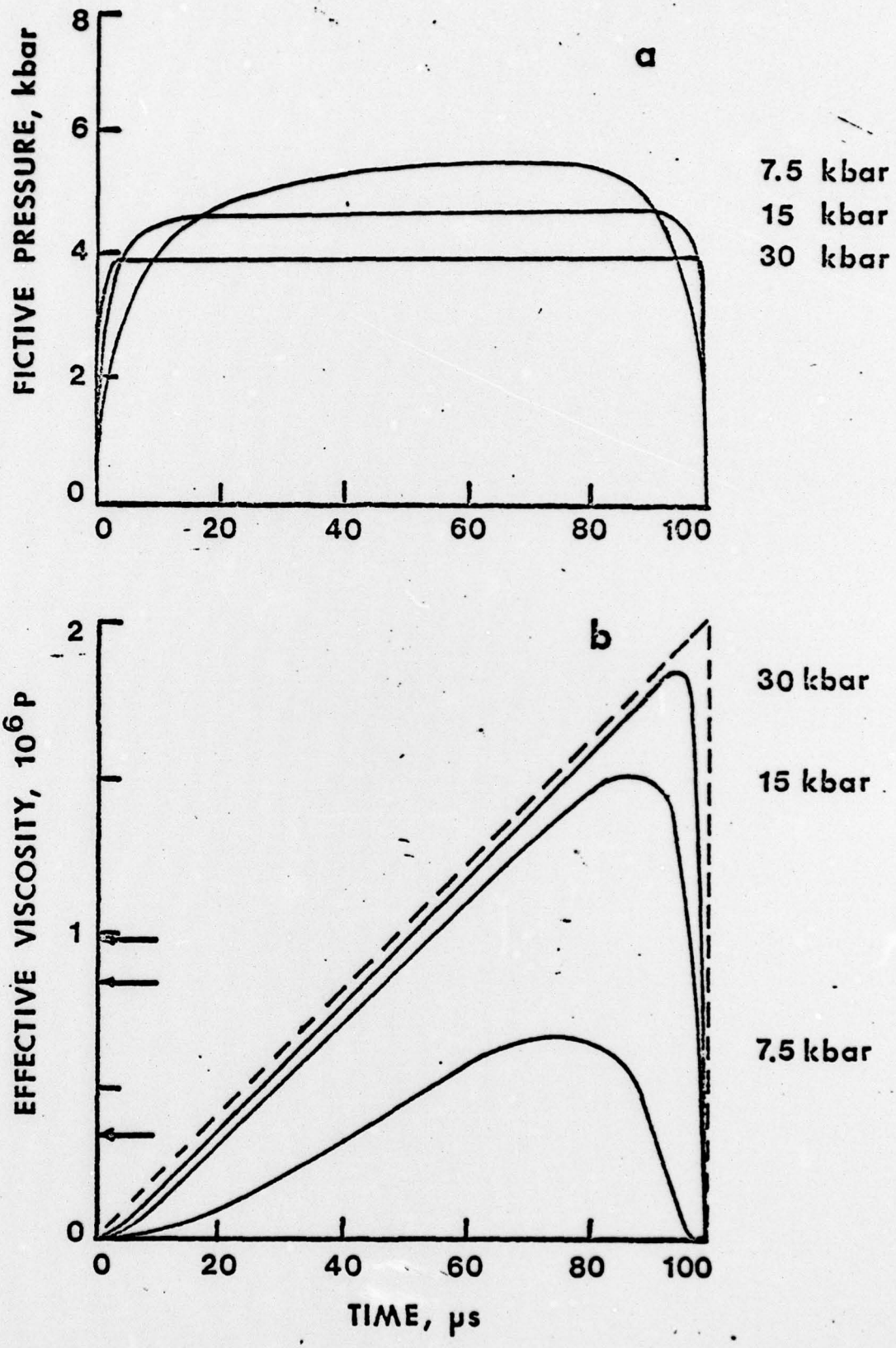
a
FICTIVE PRESSURE, kbar
8
6
4
2
0
0
20
40
60
80
100
7.5 kbar
15 kbar
30 kbar
b
EFFECTIVE VISCOSITY, 10^6 P
2
1
0
0
20
40
60
80
100
TIME, μs
30 kbar
15 kbar
7.5 kbar

FIGURE 10

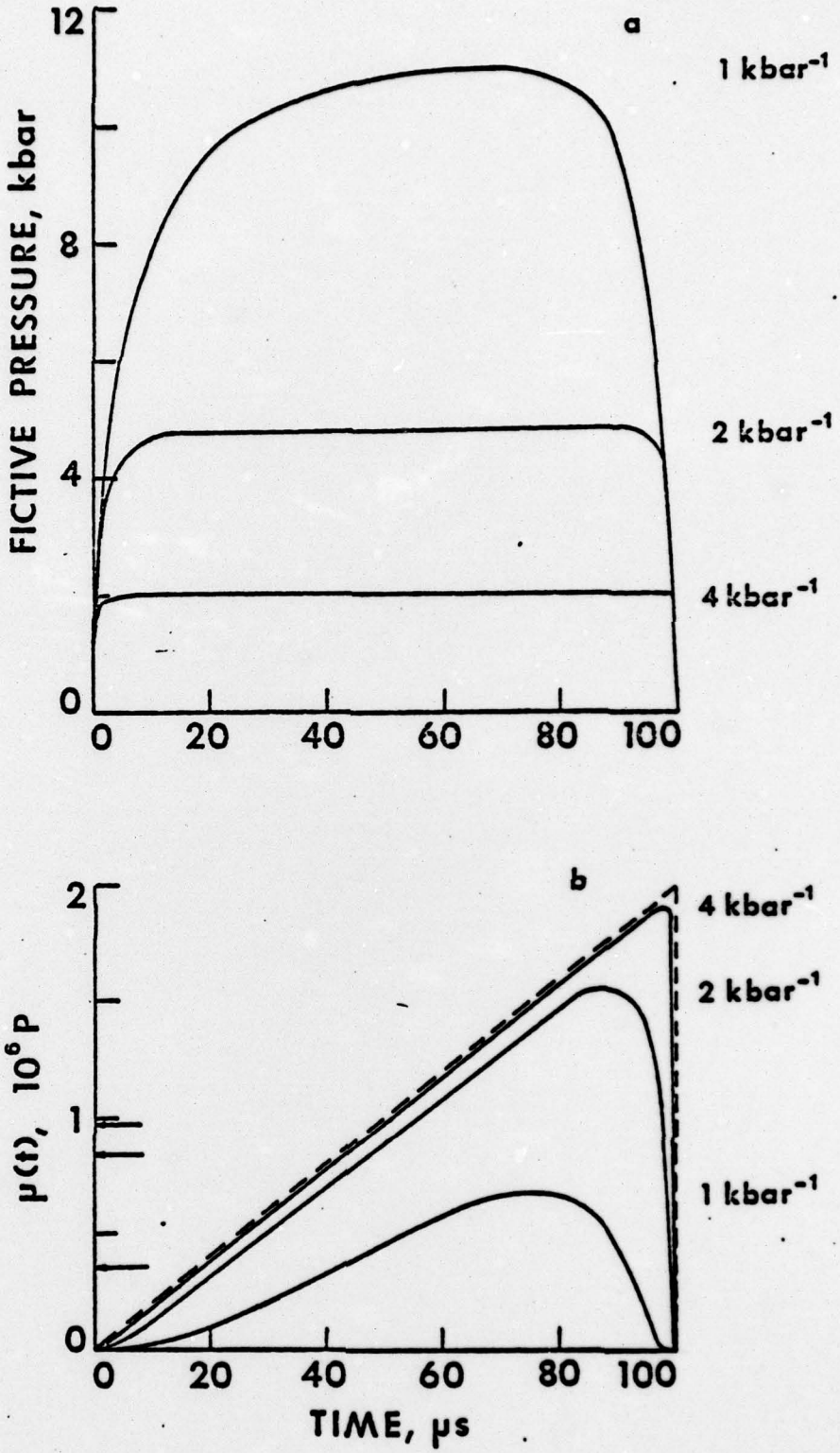
a
12
8
4
0
FICTIVE PRESSURE, kbar
0
20
40
60
80
100
1 kbar⁻¹
2 kbar⁻¹
4 kbar⁻¹
b
2
1
0
μ(t), 10⁶ P
0
20
40
60
80
100
TIME, μs
4 kbar⁻¹
2 kbar⁻¹
1 kbar⁻¹

FIGURE 11

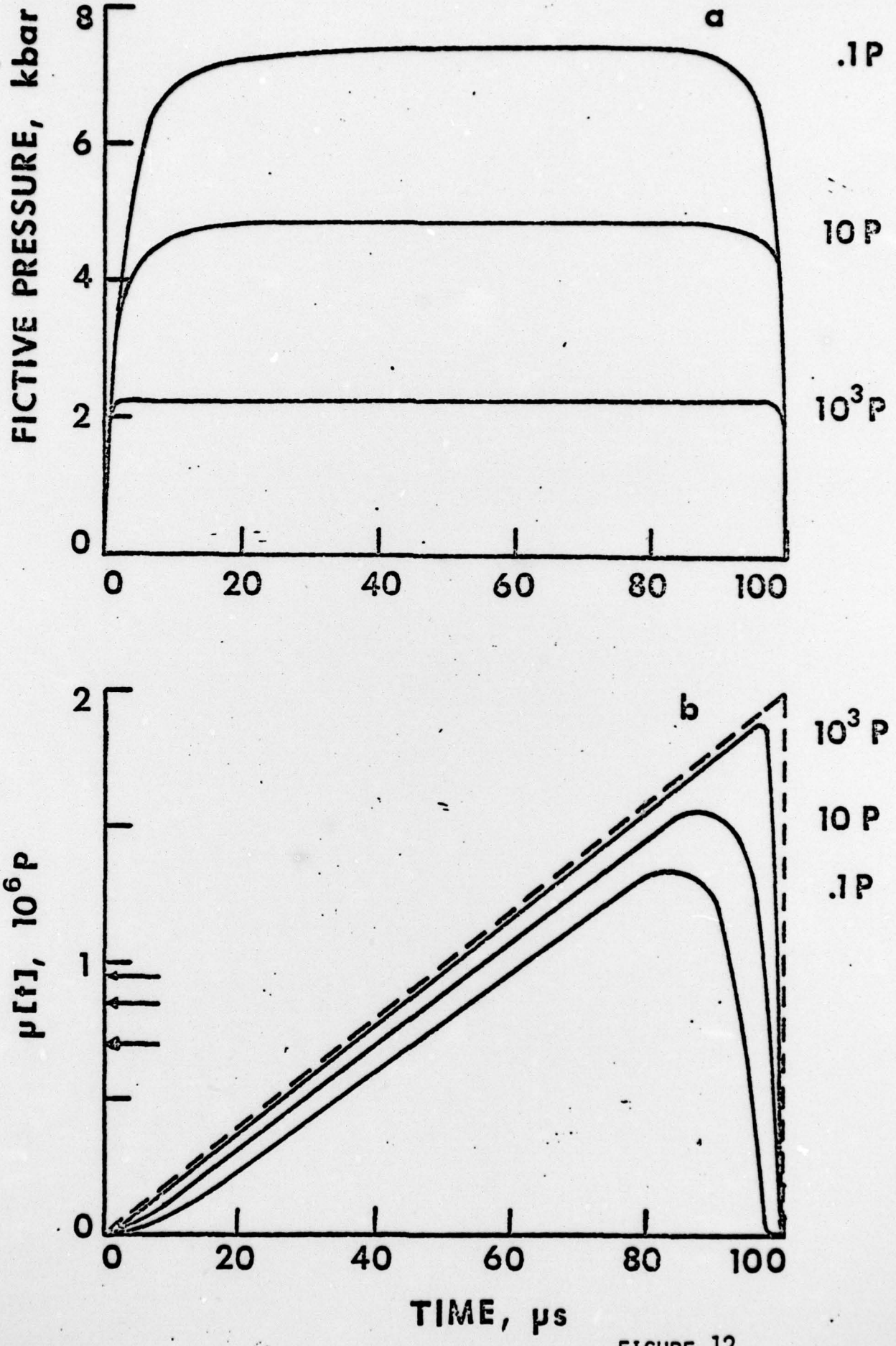
a
FICTIVE PRESSURE, kbar
8
6
4
2
0
0
20
40
60
80
100
.1P
10 P
10³P
b
μ[t], 10⁶P
2
1
0
10³ P
10 P
.1P
TIME, μs

FIGURE 12

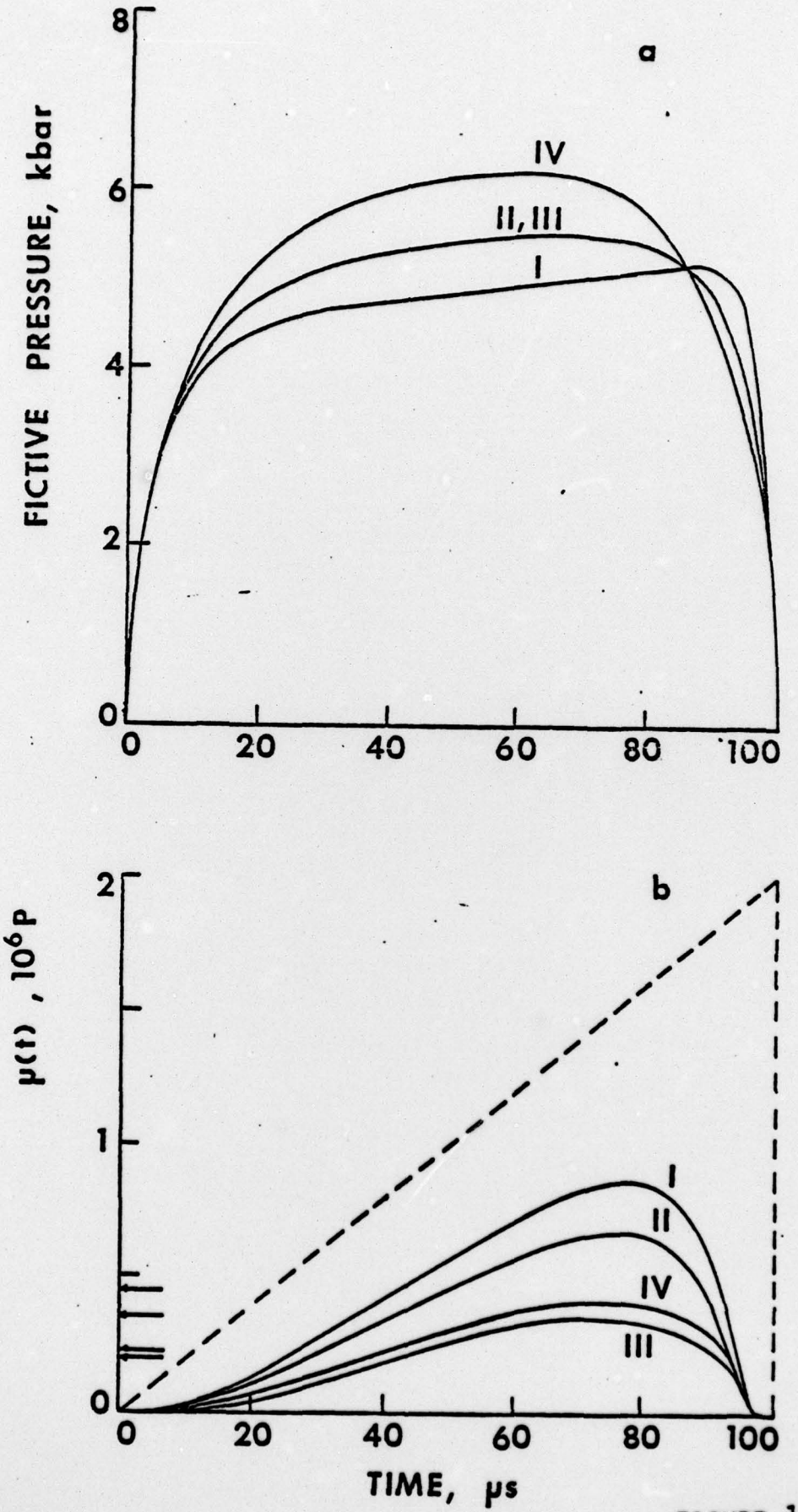
a
FICTIVE PRESSURE, kbar
8
6
4
2
0
IV
II, III
I
0
20
40
60
80
100
b
μ(t) , 10⁶P
2
1
0
I
II
IV
III
0
20
40
60
80
100
TIME, μs

FIGURE 13